BRL

AD

MEMORANDUM REPORT NO. 1915

SUPERSONIC WIND TUNNEL TESTS OF THE THREE-STAGE TARGET MISSILE ARPAT

by

Joseph M. Hughes

March 1968

U. S. ARMY MATERIEL COMMAND
BALLISTIC RESEARCH LABORATORIES
ABERDEEN PROVING GROUND, MARYLAND

B A L L I S T I C R E S E A R C H L A B O R A T O R I E S

MEMORANDUM REPORT NO. 1915

MARCH 1968

SUPERSONIC WIND TUNNEL TESTS OF THE THREE-STAGE TARGET MISSILE ARPAT

Joseph M. Hughes

Exterior Ballistics Laboratory

RDT&E Project No. 1T222901A201

A B E R D E E N P R O V I N G G R O U N D, M A R Y L A N D

TABLE OF CONTENTS

LIST OF ILLUSTRATIONS

LIST OF TABLES

LIST OF SYMBOLS

d	diameter of first stage = 1.24
ℓ	rolling moment about model axis
m	pitching moment about reference point
n	yawing moment about reference point
q	dynamic pressure = $1/2\rho V^2$
$x_{c.p.}$	distance in calibers from a point 13.5 in. aft of the nose to the center of pressure location
C_{D_A}	total indicated axial force coefficient = D_A/qS
$C_{D_{A_F}}$	fore axial force coefficient = $C_{D_A} - C_{D_{A_b}}$
$C_{D_{A_b}}$	base axial force coefficient $\frac{P_{ts} - P_{mb}}{q}$
C_m	pitching moment coefficient = $\frac{m}{qSd}$ (referred to a point 13.5 in. aft of model nose)
C_{m_α}	pitching moment coefficient slope, 1/deg
C_N	normal force coefficient, N/qS
C_{N_α}	normal force coefficient slope, 1/deg
C_ℓ	rolling moment coefficient, $\frac{\ell}{qSd}$
C_Y	side force coefficient, $\frac{Y}{qS}$
C_n	yawing moment coefficient, $\frac{n}{qSd}$
M	Mach number
N	normal force
P_{mb}	model base pressure

LIST OF SYMBOLS (CONTINUED)

P_{ts}	test section static pressure
P_o	tunnel stagnation pressure
Re/ℓ	Reynolds number per inch = $\rho V/\mu$
S	reference area = $\pi d^2/4$
T_o	stagnation temperature
V	flow velocity in test section
Y	side force
α	angle of attack of the model
ρ	air density in test section
μ	air viscosity

I. INTRODUCTION

Wind tunnel tests were performed on a four-percent scale model of the ARPAT Target Vehicle in the Ballistic Research Laboratories' (BRL) Supersonic Wind Tunnels, Aberdeen Proving Ground, Maryland, at the request of the Aerolab Development Company and the Hughes Aircraft Company. The tests were required in order to determine the final configuration and the aerodynamic parameters necessary to compute the vehicle trajectory. The important configuration elements to be determined were fin size and fin cant angle.

The test configuration consisted basically of a cone cylinder with cruciform fins having a trapezoidal planform. Two Recruit rocket motors, which were required on the prototype, were simulated between the fins at the base of the model. The size and angle of incidence of these fins were varied and the model rolled to several positions while measuring six component force data at each of four Mach numbers. These same configurations were allowed to spin freely at the same four Mach numbers in an attempt to determine the dynamic roll rate of the missile.

The models were tested at Mach numbers of 2.00, 2.50, 3.00 and 4.50 through an angle of attack range of plus 10 degrees to minus 5 degrees and at roll positions of 0, 45 and 90 degrees. The results of these tests are presented as coefficients in both tabulated and plotted form. Summary graphs of the aerodynamic coefficients plotted against Mach number are also included and discussed.

II. MODELS AND APPARATUS

The BRL Supersonic Wind Tunnels are continuous flow, closed circuit, variable density-type tunnels having flexible nozzles. These tunnels are calibrated for a Mach number range of about 1.25 to 5.00. The four-percent scale model used in the wind tunnel was over 19 in. long. To eliminate interference caused by the bow shock being reflected back onto

the model tail section, the 15 in. x 20 in. test section (Tunnel No. 3) was used for the lowest Mach number tested (2.0) and the 13 in. x 15 in. test section (Tunnel No. 1) for the higher Mach numbers.

The test configuration was basically a cone cylinder with a cruciform tail assembly. The base diameter of the cone, being larger than the mid-body cylinder, was joined to the mid-body by a cone frustrum. In the same manner, the mid-body was connected with the larger diameter aft-body cylinder. The swept, clipped tip, delta fins which form the tail assembly had a trapezoidal planform and a single wedge profile section. Four of these fin assemblies were used, providing variations of fin area and fin incidence to the airstream. The scaled 6 sq ft fin had cant angles of 15 min, 32 min, and 1 degree. The scaled 8 sq ft fin was canted at 34 min to the airstream.

Two four-percent scale models of the Recruit missile were mounted on the sides of the wind tunnel model between the tail fins and 180 degrees apart. These can be seen in Figure 1, which is a photograph of the wind tunnel model. Figure 2 also shows this configuration installed in tunnel No. 3. Model dimensions may be obtained from Figure 3, a sketch of the vehicle, or from Figure 4 which contains the fin details.

The model design was such that the same model could be used for both the force and the spin test. The spin configuration was mounted on a blank strut using precision ball bearings and allowed to spin freely, powered only by the force of the air against the canted fin. Readings of the terminal spin rate were obtained by the use of a Strobotac.

The model nomenclature is listed in Table I.

A six component internal strain gage balance was used to measure normal and side forces on the model at two axially separated positions, as well as a drag force and a rolling moment. The details of this balance are shown in the photograph, Figure 5, and in the schematic drawing, Figure 6. The model base pressure was transmitted through tubing along the sting support to a pressure transducer outside the test section.

Table I. Model Nomenclature

B_1	Body used on spin test
B_2	Body used on force test
F_6	Scaled 6 sq ft fin
F_8	Scaled 8 sq ft fin
δ_{34}	34 min fin cant angle - used on F_8
δ_1	32 min fin cant angle - used on F_6
δ_4	1 degree fin cant angle - used on F_6
δ_2	15 min fin cant angle - used on F_6 (spin model only)
R_o	Model roll position, $\phi = 0$ degrees
R_{45}	Model roll position $\phi = 45$ degrees
R_{90}	Model roll position $\phi = 90$ degrees

The automatic data readout system, which is used in conjunction with wind tunnel tests, records the raw data in tabulated, punched tape and plotted form. In this system the forces and moments generated by the air flowing over the model are transmitted to the strain gage balance. The strain gage bridge output is used to actuate a servo type follow up system which translates this millivolt signal into an output shaft position. This, in turn, is converted into an electrical input for the Flexowriter, tape punch and plotter systems and provides a direct angular input to the syncro-indicating system.

During the course of a test run, the angle that the model makes with the airstream in the pitch plane is changed continuously at the rate of 1 degree in 8 seconds, and a cam on the angle of attack system automatically initiates a reading for each degree of travel. The accuracy of the system is $\pm$ 0.02 percent of the full scale reading.

III. TEST PROCEDURE

The test configuration was installed on the tunnel centerline and rotated through angles of attack in the pitch plane from plus 10 degrees to minus 5 degrees. The force test was conducted in the following manner:

a. With the model level in the tunnel, flow was established at the proper Mach number, but at a greatly reduced stagnation pressure.

b. The stagnation pressure was then increased to the test condition and six component force data and a base pressure reading were recorded at 0 degree angle of attack.

c. After increasing the angle of attack to 10 degrees, data were recorded and plotted as the angle of attack was decreased from plus 10 degrees to minus 5 degrees.

d. Schlieren photographs were taken at 0 degree and 6 degrees for all runs. Additional photographs were taken as required, to record flow changes about the model.

e. The stagnation pressure was reduced before shutting down the system.

This procedure was followed for each of the four sets of fins, at each of three roll positions, and at each of four Mach numbers. By definition, the zero roll position was that position when the plane containing the two Recruits was parallel to the tunnel floor.

To determine the roll rate of the model, each of the canted fin configurations was allowed to spin freely in the airstream at each of three Mach numbers. The terminal spin frequency was then obtained by the use of a Stroboscope.

The tunnel operating conditions are recorded in Table II.

Table II. Tunnel Operating Conditions

M	P_o cm Hg abs	q psi	$Re/\ell \times 10^{-6}$ per inch
2.00	99	6.82	.40
2.50	130	6.41	.40
3.00	162	5.35	.40
4.50	327	3.08	.40

The specific humidity of the air in the tunnel was kept below 0.0002 pound of water per pound of air.

IV. DATA REDUCTION

The data reduction equations were programmed for the electronic computer (BRLESC) and the aerodynamic coefficients were obtained by the Computing Laboratory, BRL.

The angle of attack of the model in the tunnel was corrected for the deflection of the strut under load. These deflection constants were obtained by a calibration which consisted of subjecting the model and model support system in the tunnel to known loads at predetermined locations.

To make a first order correction for the effect of tunnel flow inclination in the region of the test section, the normal force and pitching moment curves have been translated so that they pass through the origin, i.e., zero angle of pitch. This was done by the computer in the following manner:

a. The curve of normal force vs. angle of attack was moved along the angle of attack axis to the origin. The angle through which the curve was moved was usually less than $\pm$ 0.1 degree.

b. The pitching moment was plotted against this corrected angle of attack and then moved along the pitching moment axis to the origin. The amount that this curve was translated was usually less than $\pm$ 0.2 in. lb for Mach numbers other than 2.00. The correction at Mach No. 2.00 was on the order of 2.0 in. lb.

The sting type support can affect the wake flow, and so affect the total drag, but in general the flow over the other portions of the body is not affected. The fore drag coefficients used in this report represent the drag on the complete model with the base pressure set equal to the test section static pressure. These coefficients are obtained by subtracting from the indicated drag coefficient the base drag coefficient, which is determined from base pressure measurements.

The aerodynamic coefficients and parameters presented in this report are believed to be internally consistent for any one run within the approximate values set forth in Table III.

Table III. Data Accuracy

M	α deg	C_N	C_m	$C_{D_{A_F}}$	C_n	C_Y	C_ℓ
2.00	.05	.01	.01	.02	.01	.01	.01
2.50	.05	.01	.01	.01	.01	.01	.01
3.00	.05	.01	.01	.01	.01	.01	.01
4.50	.05	.02	.02	.02	.02	.02	.01

The centers of pressure are accurate to within 0.20 calibers for all tests using the equation

$$c.p. = \frac{dC_m/d\alpha}{dC_N/d\alpha}$$

where slopes were taken between plus or minus 2 degrees angle of attack. For all other angles the center of pressure positions are accurate to

within 0.10 calibers using point by point calculation where

$$c.p. = C_m/C_N.$$

The force and moment coefficients have been referred to a body axis system through a point 13.5 in. downstream from the tip of the nose and on the longitudinal centerline of the model. The center of pressure positions (x_{cp}) were also measured from this point and a positive value of x_{cp} indicates that the cp is forward of the reference point. The coefficients have been computed using the relationships given in the "List of Symbols" with the reference diameter and area being that of the first stage of the missile.

V. RESULTS

The aerodynamic coefficients are defined by the relationships given in the "List of Symbols" and are presented in both tabulated and graphical form. Table IV presents the more important aerodynamic parameters in summary form, while Figures 7 through 14 are plots of these data as a function of Mach number. The basic data in coefficient form are presented graphically as a function of angle of attack in Figures 15 through 38 for Mach numbers of 2.00, 2.50, 3.00 and 4.50.

These tests were performed primarily in order to determine the static aerodynamic stability of the model and the effect on this stability of varying fin size and fin incidence to the airstream. This information can be most easily obtained by referring to the aforementioned summary graphs, Figures 7 through 14.

The drag coefficients of the complete missile decrease about 50 percent over the Mach number range of 2.00 to 4.50. The change of fin incidence of half a degree does not change the drag coefficients (Figure 7).

Table IV. Summary of Aerodynamic Parameters

(α = 0 degrees)

M	Configuration	C_{N_α} 1/deg	C_{m_α} 1/deg	$X_{c.p.}$ Cal. fr. cg.	C_ℓ	$C_{D_{A_F}}$
2.00	$B_2\delta_1F_6R_0$	.210	.081	-0.35	.080	0.76
	$B_2\delta_1F_6R_{45}$	.204	.115	-0.58	.080	0.76
	$B_2\delta_1F_6R_{90}$	.195	.160	-0.80	.080	0.76
	$B_2\delta_4F_6R_{90}$	.198	-.144	-0.80	.145	0.78
	$B_2\delta_{34}F_8R_0$	.248	-.260	-1.03	.130	0.84
	$B_2\delta_{34}F_8R_{45}$	.248	-.300	-1.20	.130	0.84
	$B_2\delta_{34}F_8R_{90}$	.241	-.330	-1.40	.120	0.84
2.50	$B_2\delta_1F_6R_0$	.179	.015	0	.065	0.56
	$B_2\delta_1F_6R_{45}$	.170	.017	0.05	.065	0.59
	$B_2\delta_1F_6R_{90}$	.158	.022	0.10	.065	0.57
3.00	$B_2\delta_1F_6R_0$	.163	.071	0.42	.052	0.44
	$B_2\delta_1F_6R_{45}$	.156	.088	0.56	.052	0.48
	$B_2\delta_1F_6R_{90}$	.132	.110	0.79	.052	0.43
	$B_2\delta_4F_6R_{90}$	.136	.103	0.72	.086	0.46
	$B_2\delta_{34}F_8R_0$	.184	-.003	0	.073	0.47

Table IV (Continued)

M	Configuration	C_{N_α} 1/deg	C_{m_α} 1/deg	$X_{c.p.}$ Cal. fr. cg.	C_l	$C_{D_{A_F}}$
3.00	$B_2\delta_{34}F_8R_{45}$	.178	-.008	0	.073	0.49
	$B_2\delta_{34}F_8R_{90}$	.164	-.008	0	.073	0.52
4.50	$B_2\delta_1F_6R_0$	.161	.180	1.00	.033	0.37
	$B_2\delta_1F_6R_{45}$	.139	.205	1.40	.033	0.37
	$B_2\delta_1F_6R_{90}$	.127	.245	1.80	.033	0.33
	$B_2\delta_4F_6R_{90}$	.122	.227	1.75	.065	0.35
	$B_2\delta_{34}F_8R_0$	.170	.118	0.62	.055	0.39
	$B_2\delta_{34}F_8R_{45}$	.152	.140	0.80	.055	0.39
	$B_2\delta_{34}F_8R_{90}$	.144	.160	1.02	.055	0.39

These drag forces utilized, at best, only the lower 20 percent of the range of the balance, and because of unsteady flow over the tail section, they were erratic at some Mach numbers.

The normal force slope, C_{N_α}, decreases about 40 percent with an increase of Mach number from 2.00 to 4.50. The angle of fin incidence (δ_1 and δ_4) has no effect on the normal force, as one would expect, but with reduced fin size of 33 percent the normal force slope decreases about 15 percent (F_6 and F_8). See Figure 8. These results were obtained with the roll angle of the model at $\phi = 90$ degrees, i.e., having the booster rockets in the pitch plane of the model. In Figure 9 it can be seen that the normal force changes only a little with roll orientation at the low Mach numbers, but that there is an appreciable change at the higher Mach numbers. That this situation can exist when the rocket motors are fully exposed to the flow must be a result of the intricate flow patterns and consequent force interactions about the tail section.

With an increase of fin size from scaled values of 6 to 8 sq ft or 33 percent (compare $\delta_1 F_6$ and $\delta_{34} F_8$ on Figure 10), the rolling moment C_ℓ increased almost 70 percent. Tests using the same size fin but increasing the fin incidence from 32 minutes to 1 degree (δ_1 and δ_4, Figure 10) caused an increase of rolling moment of about 70 to 100 percent through the Mach number range. In contrast to this the freely spinning model test showed that the terminal spin was a direct function of fin incidence alone. See Figure 11.

The center of pressure of the model changes with fin area as would be anticipated. This c.p. travel as shown in Figure 12 is about .50 cal rearward for an increase of fin size of 33 percent. This change of fin area will also change the point of neutral stability ($x_{cp} = 0$) from a Mach number of 2.40 to a Mach number of 3.00. From Figure 13 it can be seen that the center of pressure will change as much as .75 of a caliber with roll position, while Figure 14 indicates that fin cant angle has no effect on stability.

Note that in comparing roll angles of 0 and 90 degrees, the pattern of the movement of the center of pressure and the change in C_{N_α} values with Mach number do not follow the trends that one would expect by assuming the booster rockets to be additional lifting surfaces. The flow pattern around the rockets and tail section is not simple and is prone to change with the pitch angle of the missile. Some indication of the flow intricacies may be observed in the schlieren photographs, Figures 39 through 42.

Figure 1. Photograph of wind tunnel model

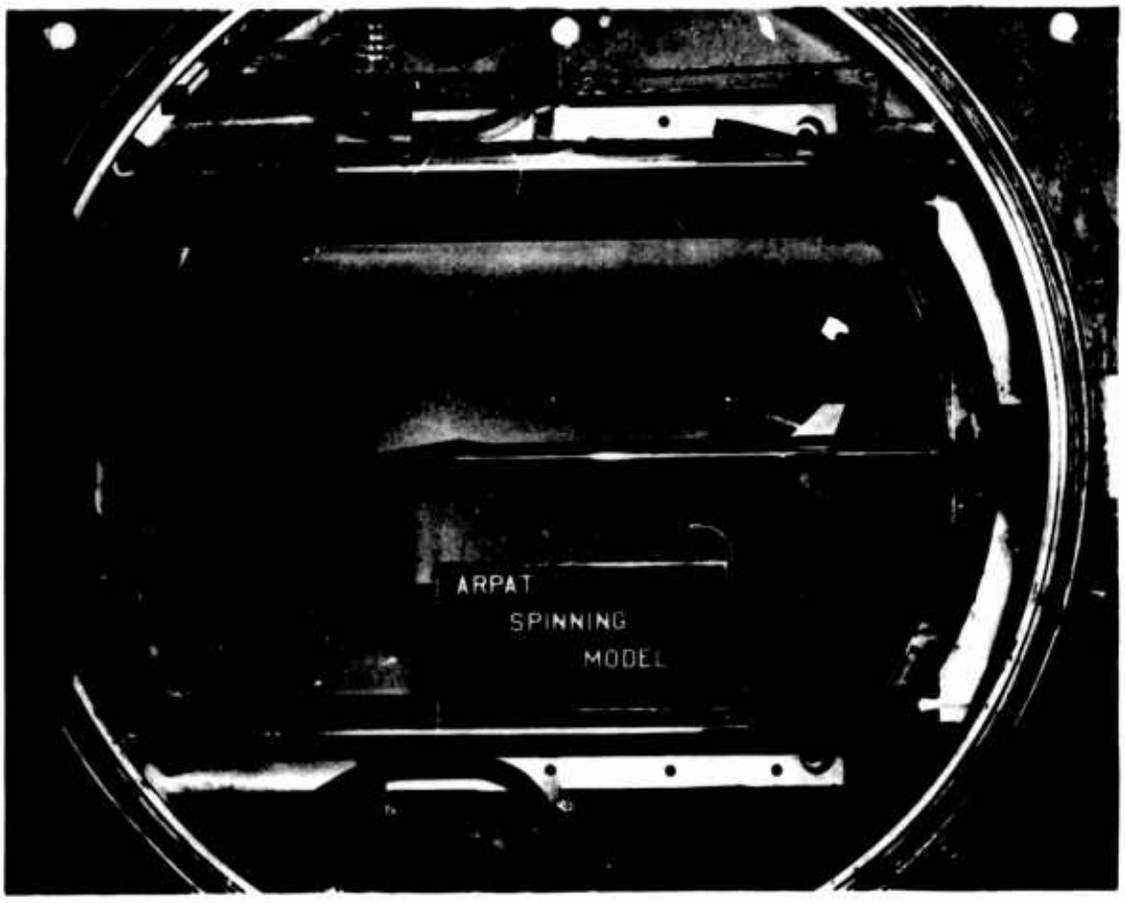

Figure 2. Photograph of model installed in the tunnel

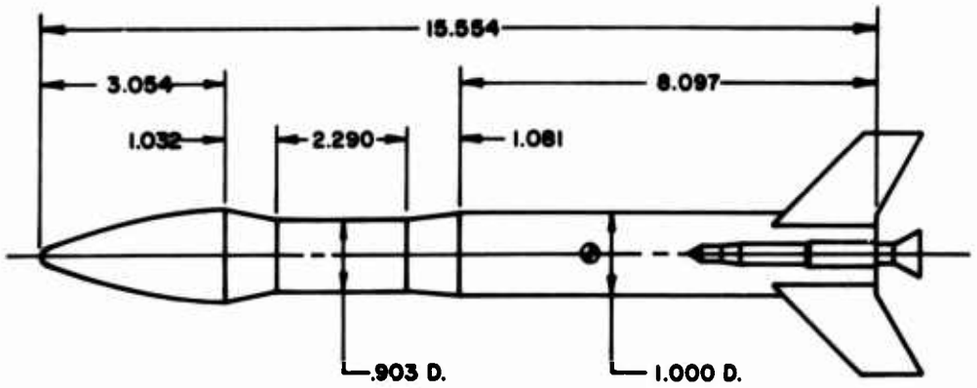

NOTE:
ALL DIMENSIONS IN CALIBERS.
1 CALIBER = 1.24"

ARPAT TARGET VEHICLE

Figure 3. Sketch of the wind tunnel model

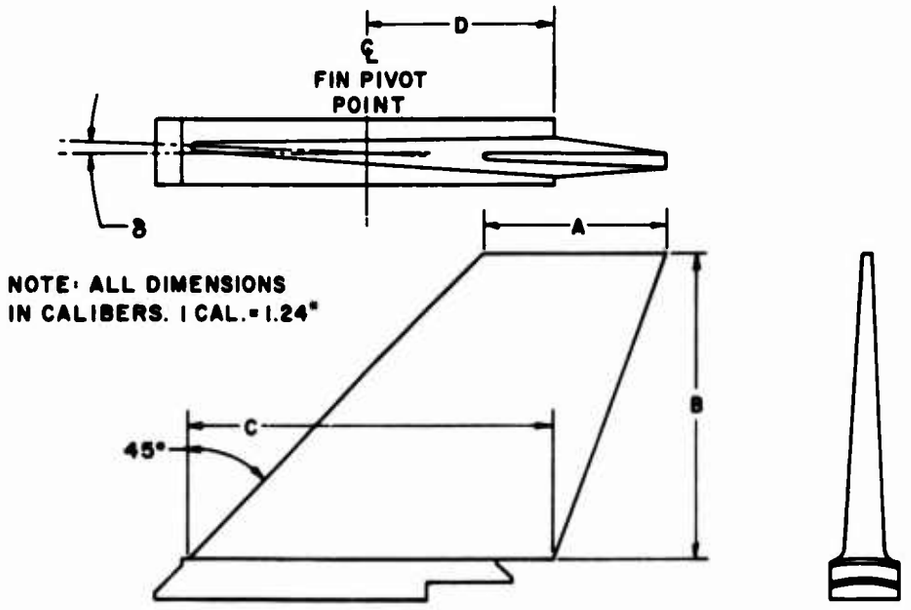

FIN	A	B	C	D
F_8	.645	.935	1.290	.645
F_8	.710	1.129	1.419	.710

Figure 4. Sketch of model fin detail

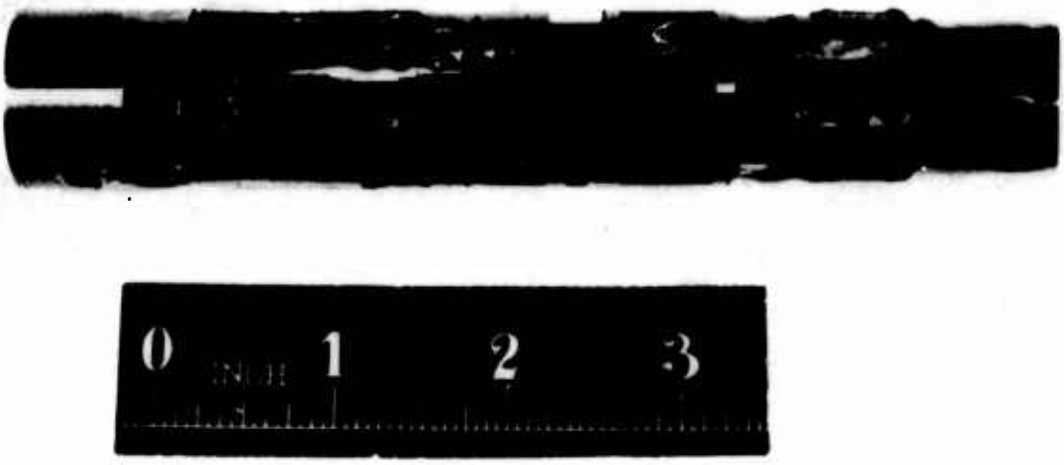

Figure 5. Photograph of the internal balance

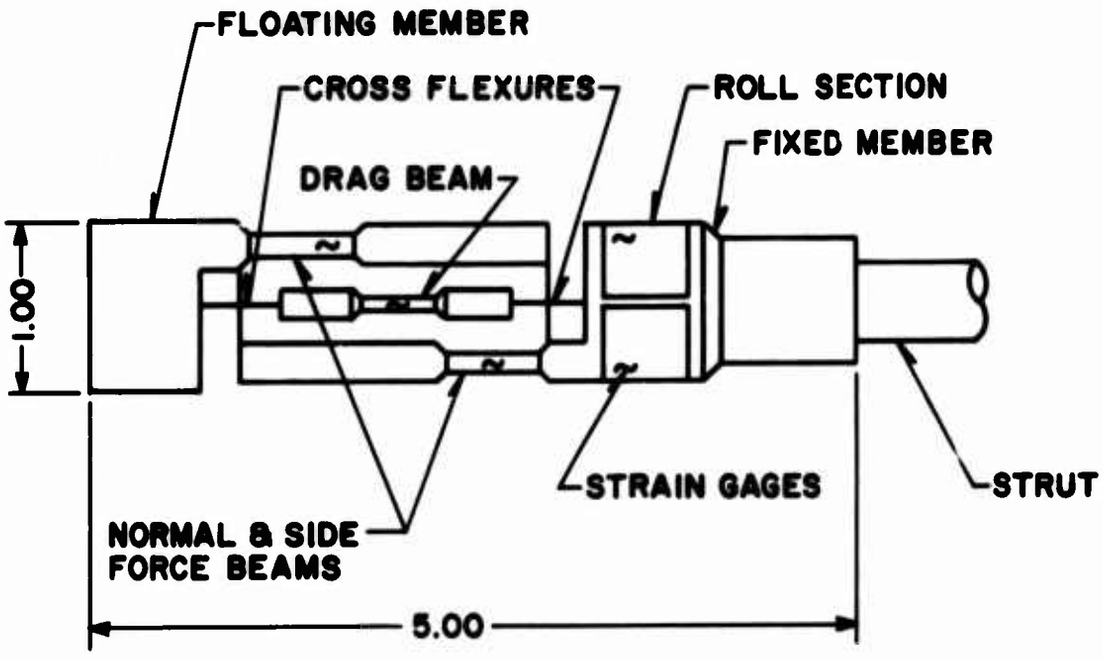

Figure 6. Schematic of the 6-component strain gage balance

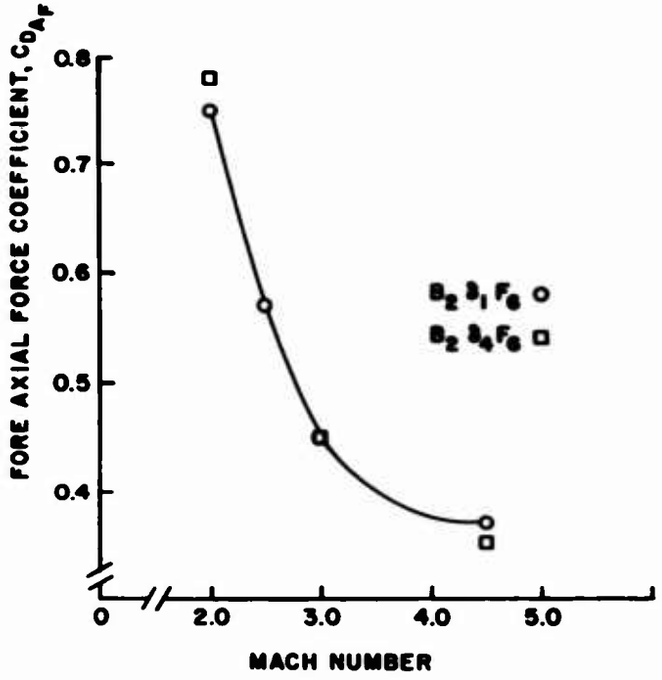

Figure 7. Fore axial force coefficient as a function of Mach number for various fin deflection angles

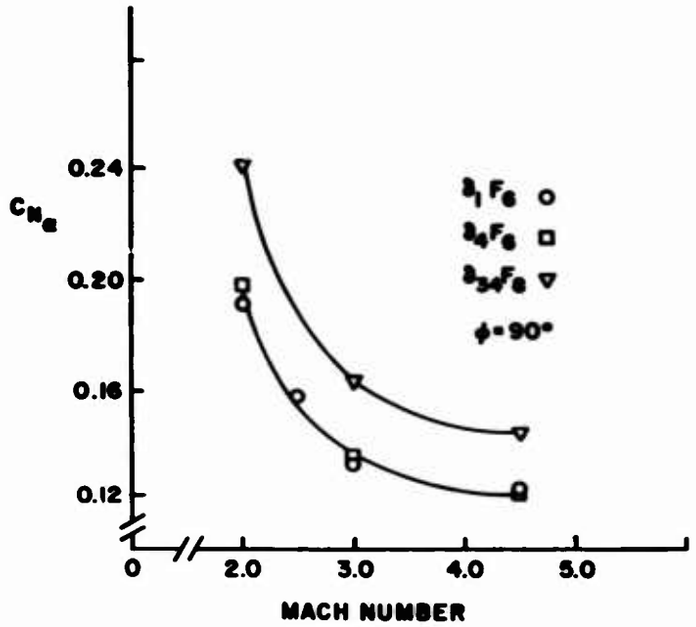

Figure 8. Normal force coefficient slope as a function of Mach number for various fin areas and fin deflection angles

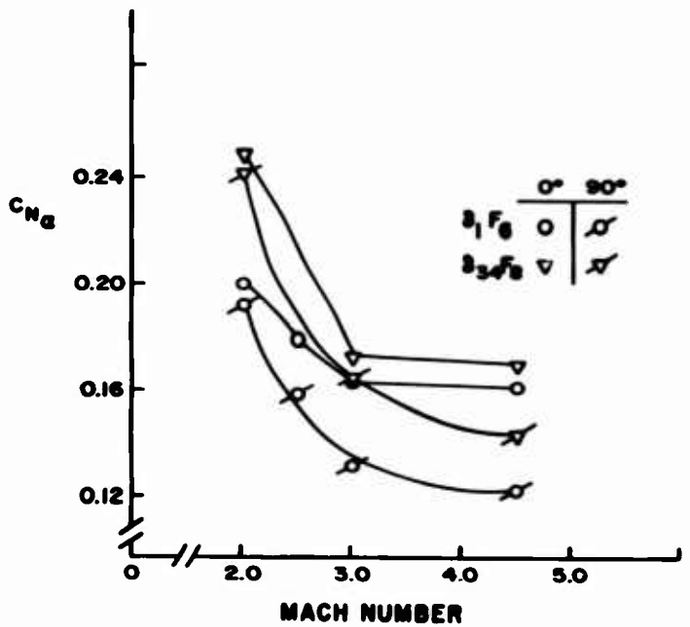

Figure 9. Normal force coefficient slope as a function of Mach number for various fin deflections and roll angles

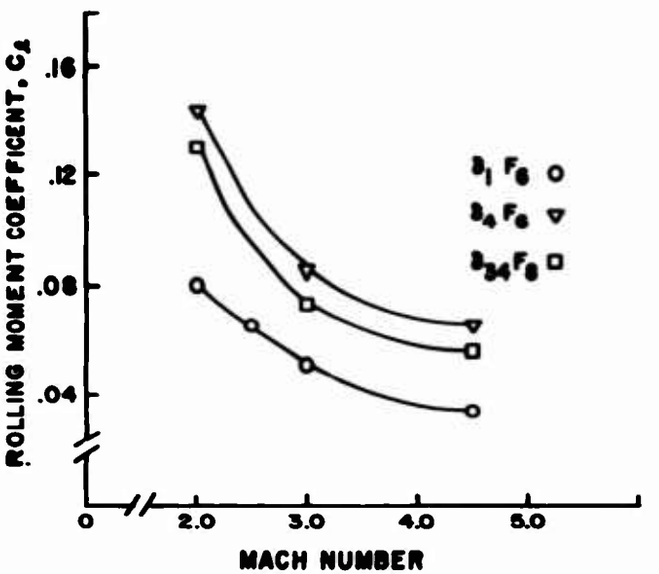

Figure 10. Rolling moment coefficient as a function of Mach number for various fin areas and angles of incidence

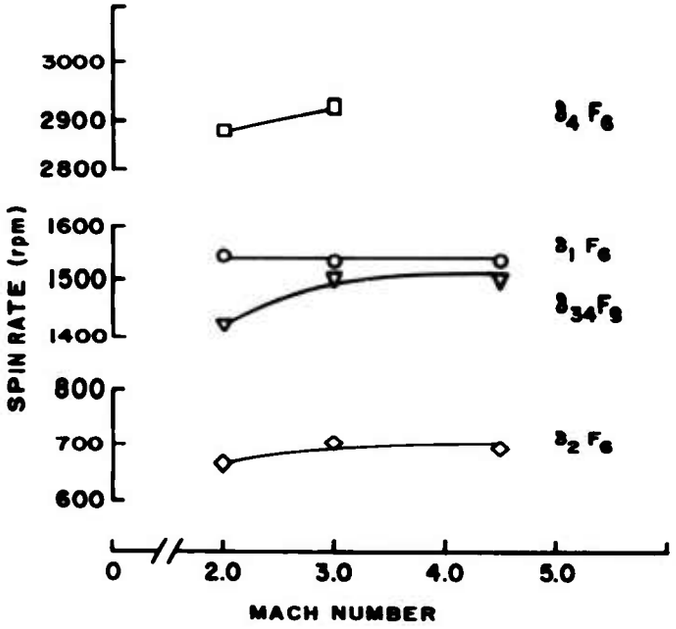

Figure 11. Spin rate as a function of Mach number for various fin areas and deflection angles

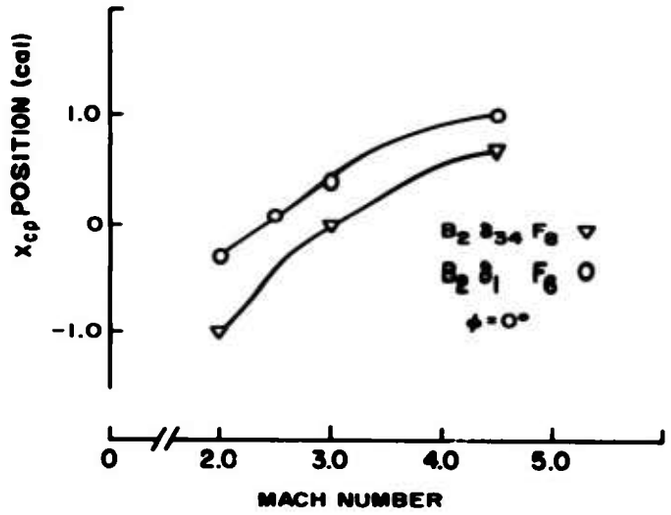

Figure 12. Static stability as a function of Mach number for various fin areas

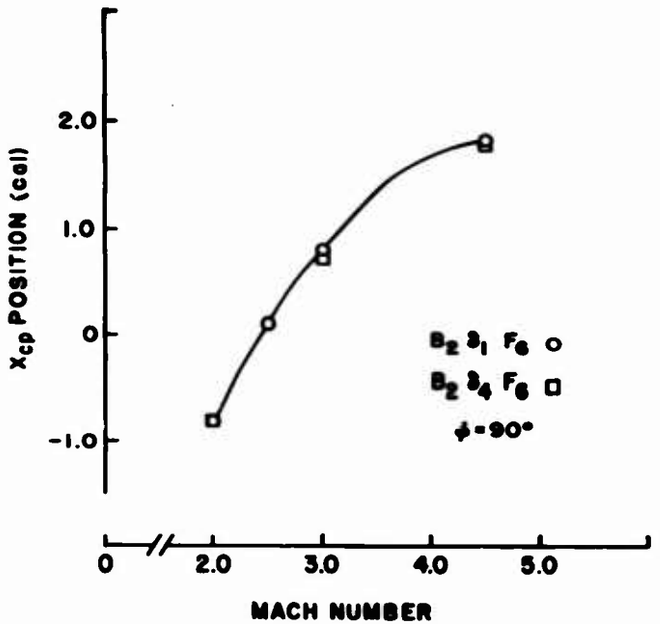

Figure 13. Static stability as a function of Mach number for each of three model roll positions

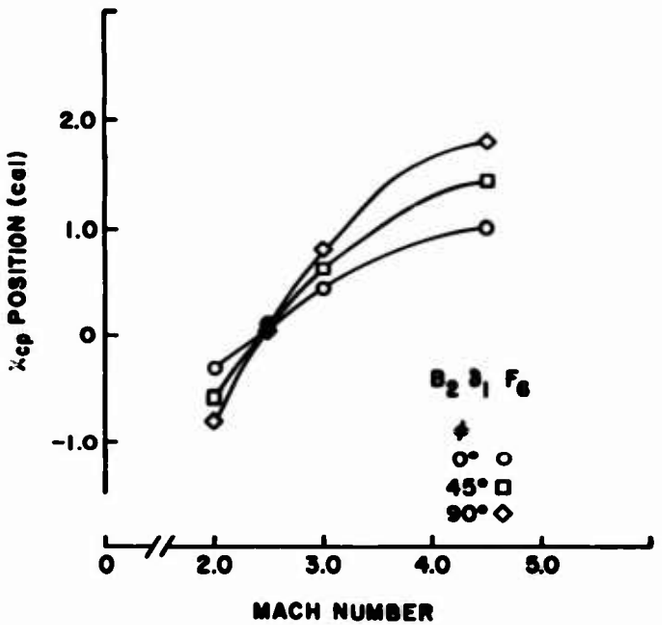

Figure 14. Static stability as a function of Mach number for two fin deflection angles at ϕ = 90°

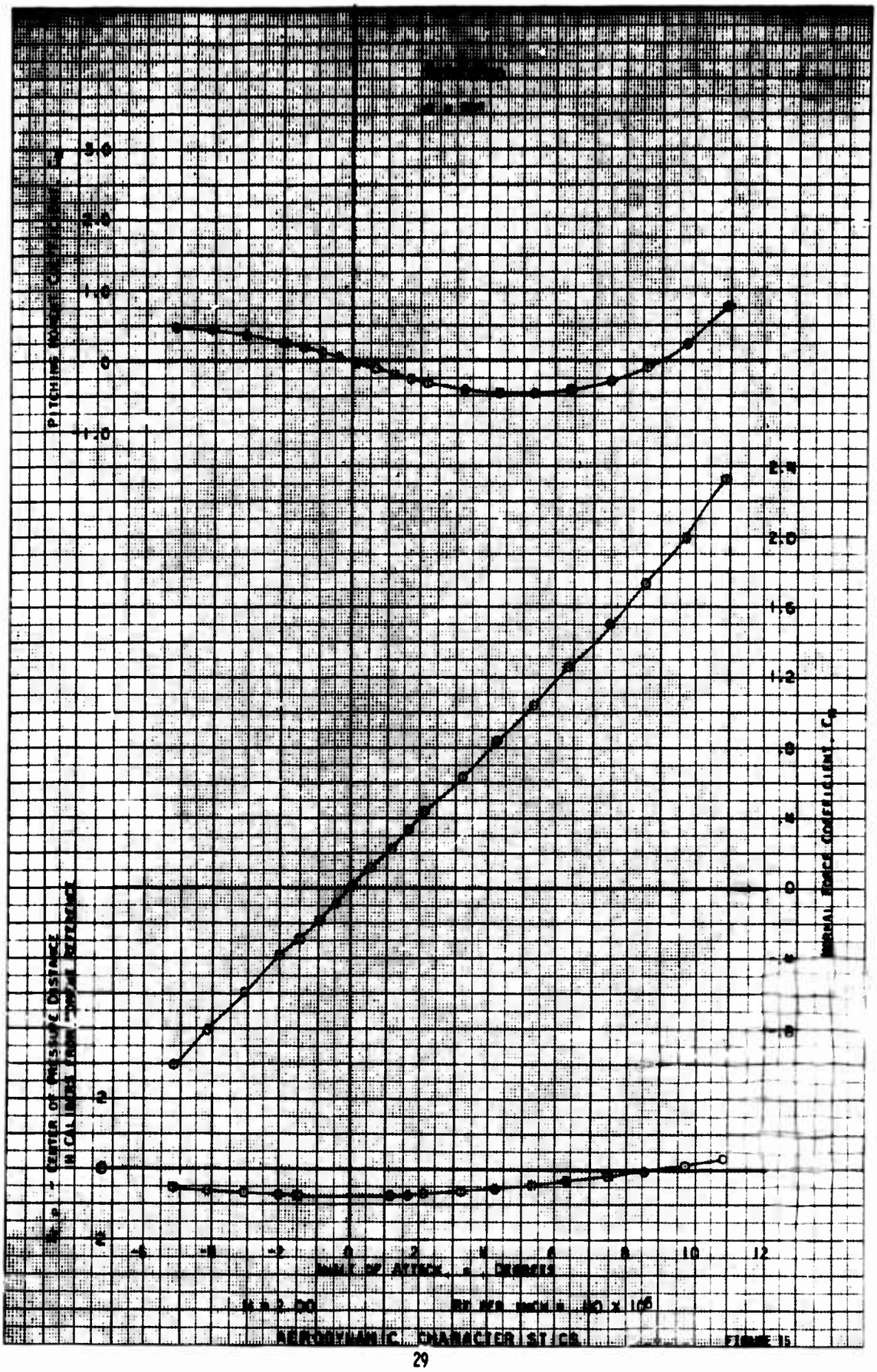
PITCHING MOMENT COEFFICIENT, C_m
$\frac{x_{cp}}{c}$ = CENTER OF PRESSURE DISTANCE
INCHES FROM LEADING EDGE
NORMAL FORCE COEFFICIENT, C_n
ANGLE OF ATTACK, α, DEGREES
M = 2.00
RE PER INCH = 10 x 10⁶
AERODYNAMIC CHARACTERISTICS
FIGURE 15

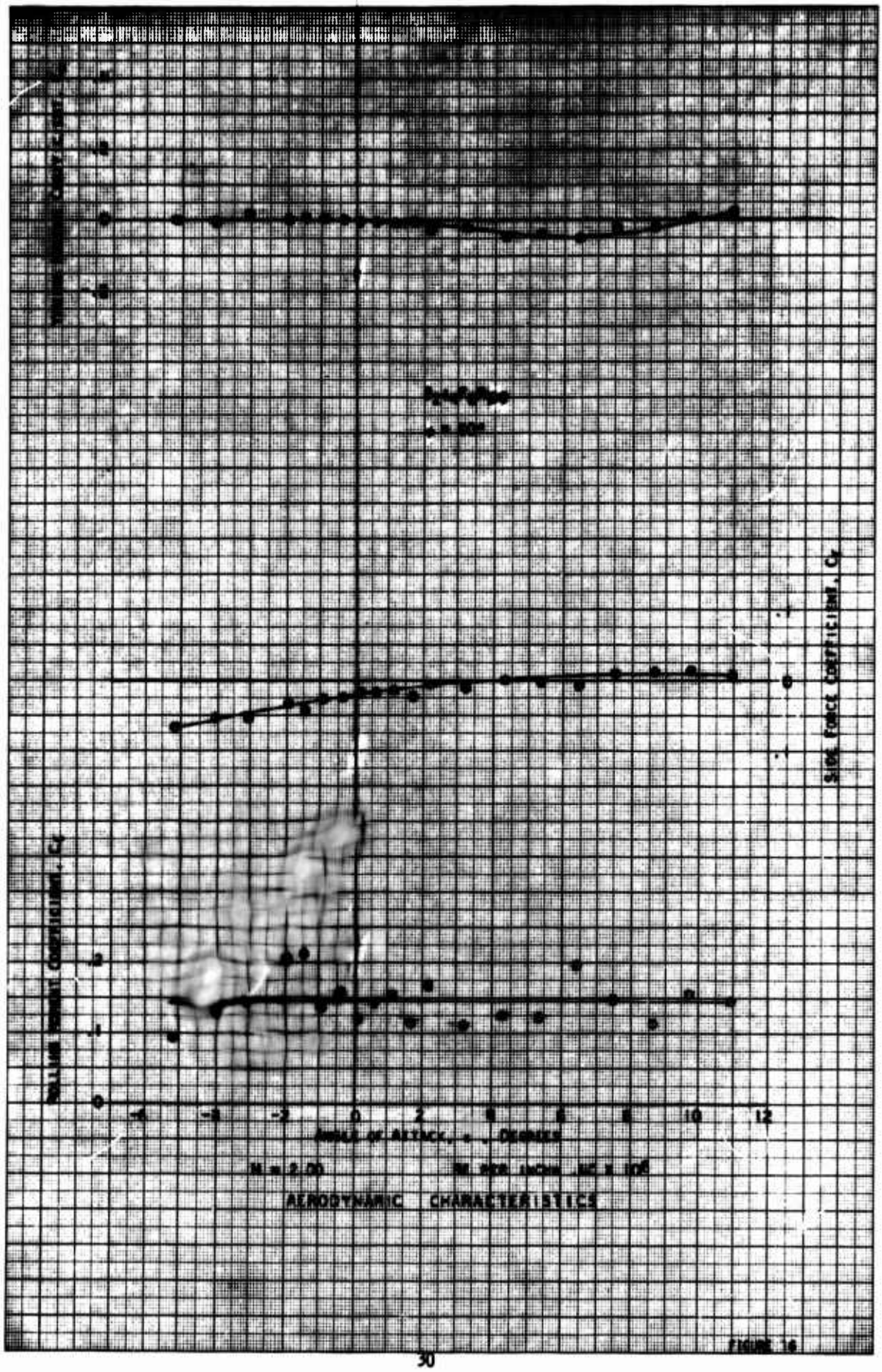
Side force coefficient, C_Y
Rolling moment coefficient, C_l
Angle of attack, α, degrees
M = 2.00
Re per inch, RC x 10⁶
AERODYNAMIC CHARACTERISTICS

FIGURE 16

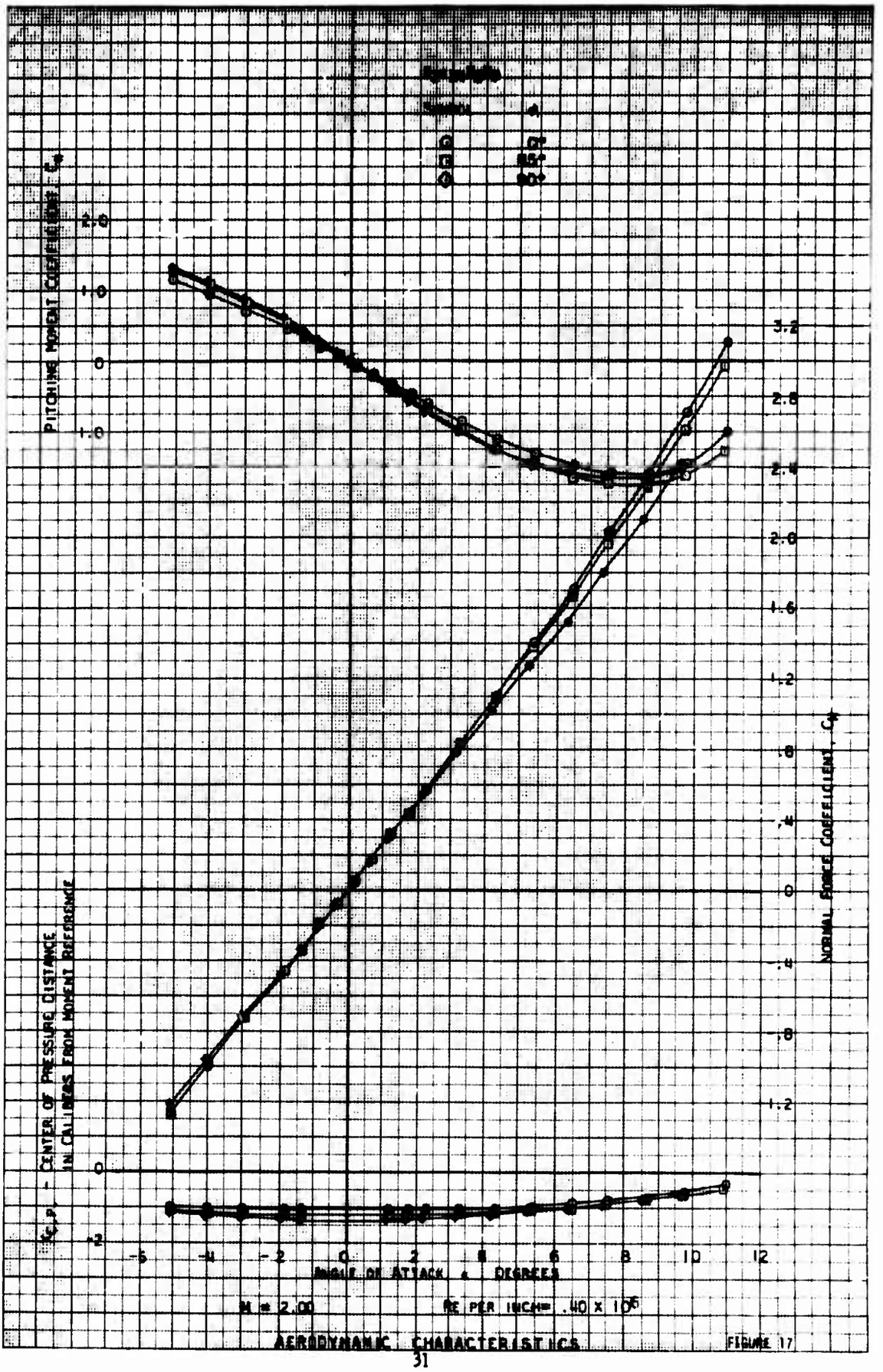

AERODYNAMIC CHARACTERISTICS

FIGURE 17

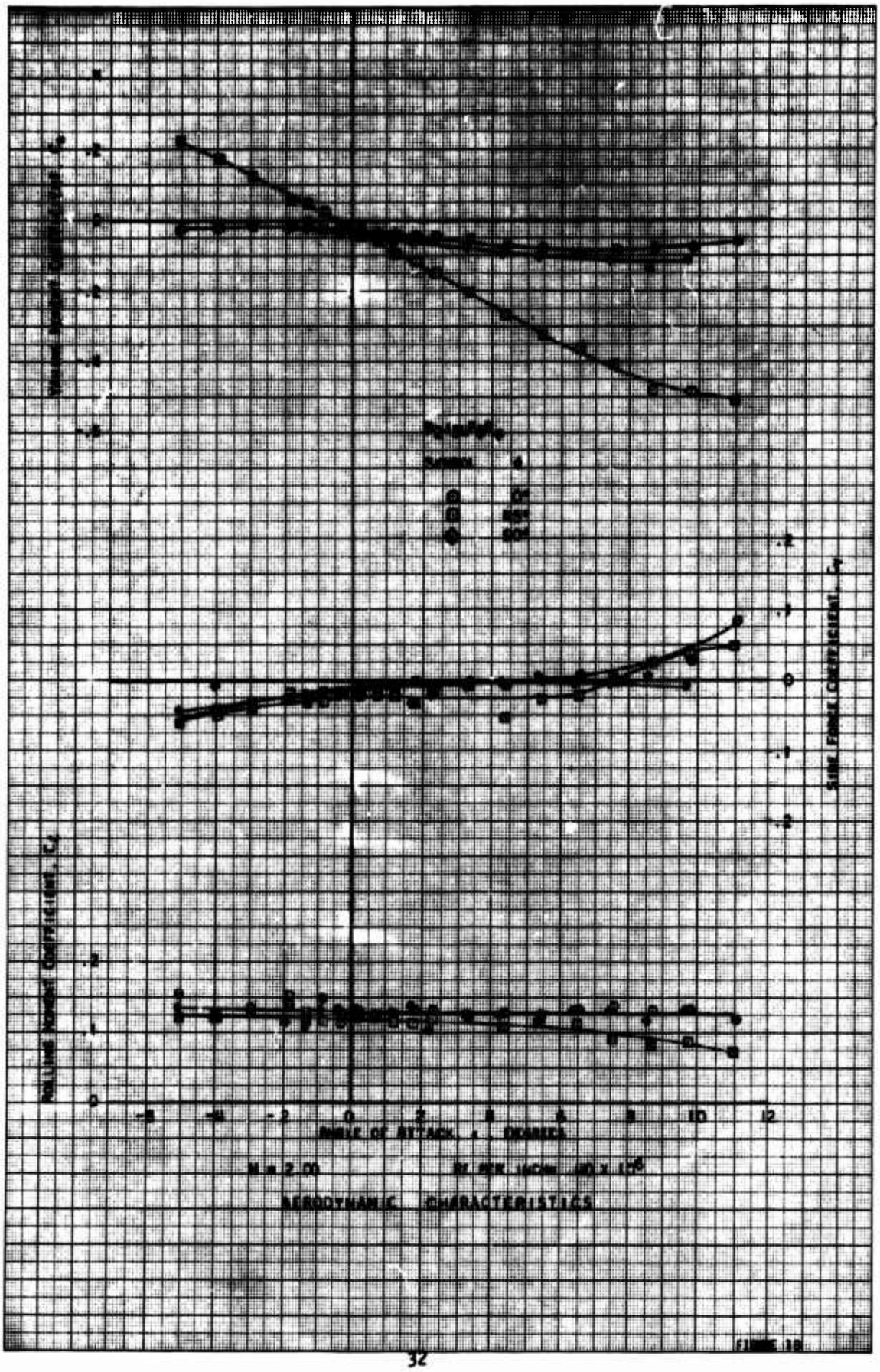
ANGLE OF ATTACK, α, DEGREES
AERODYNAMIC CHARACTERISTICS

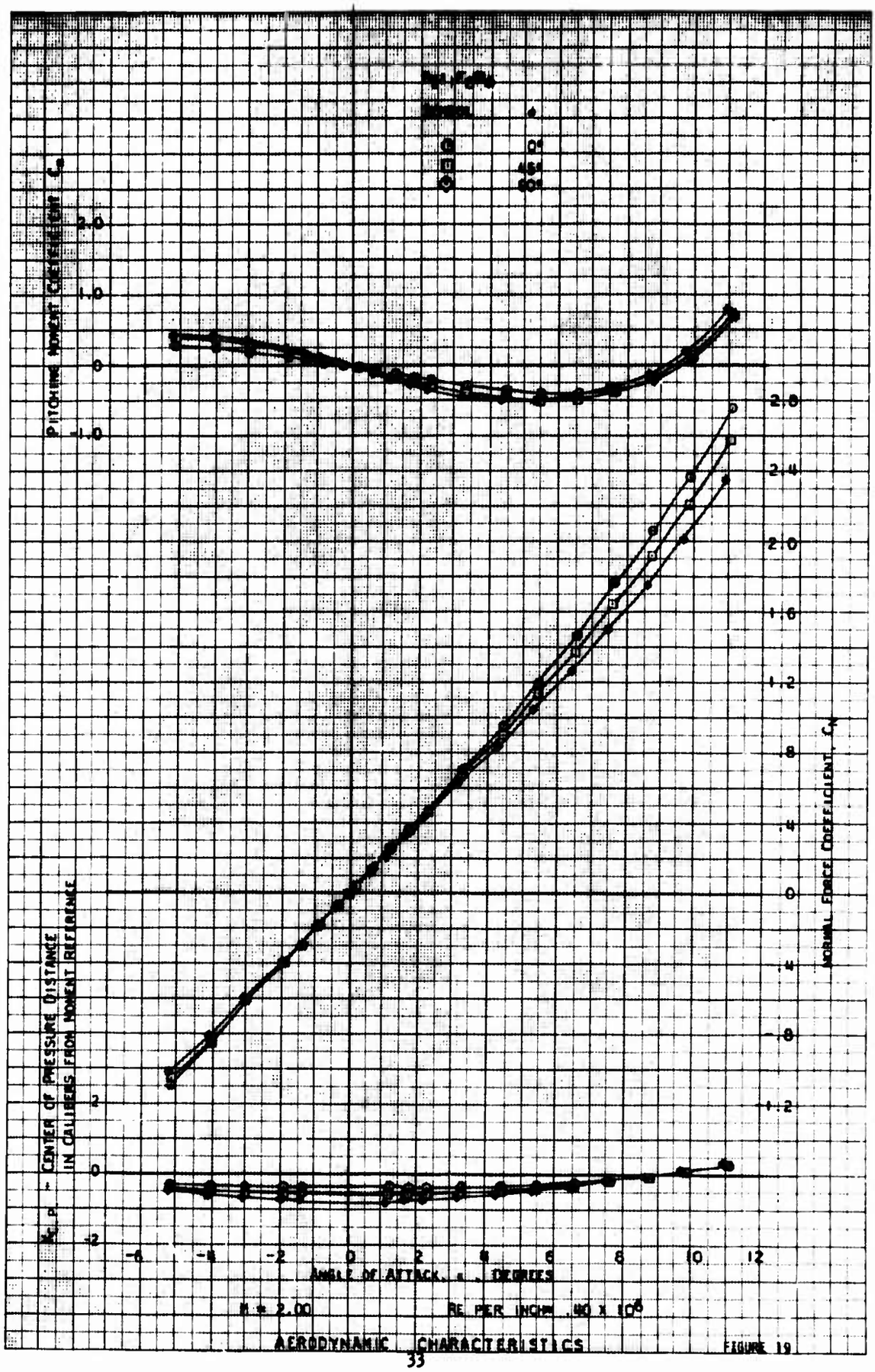

AERODYNAMIC CHARACTERISTICS FIGURE 19

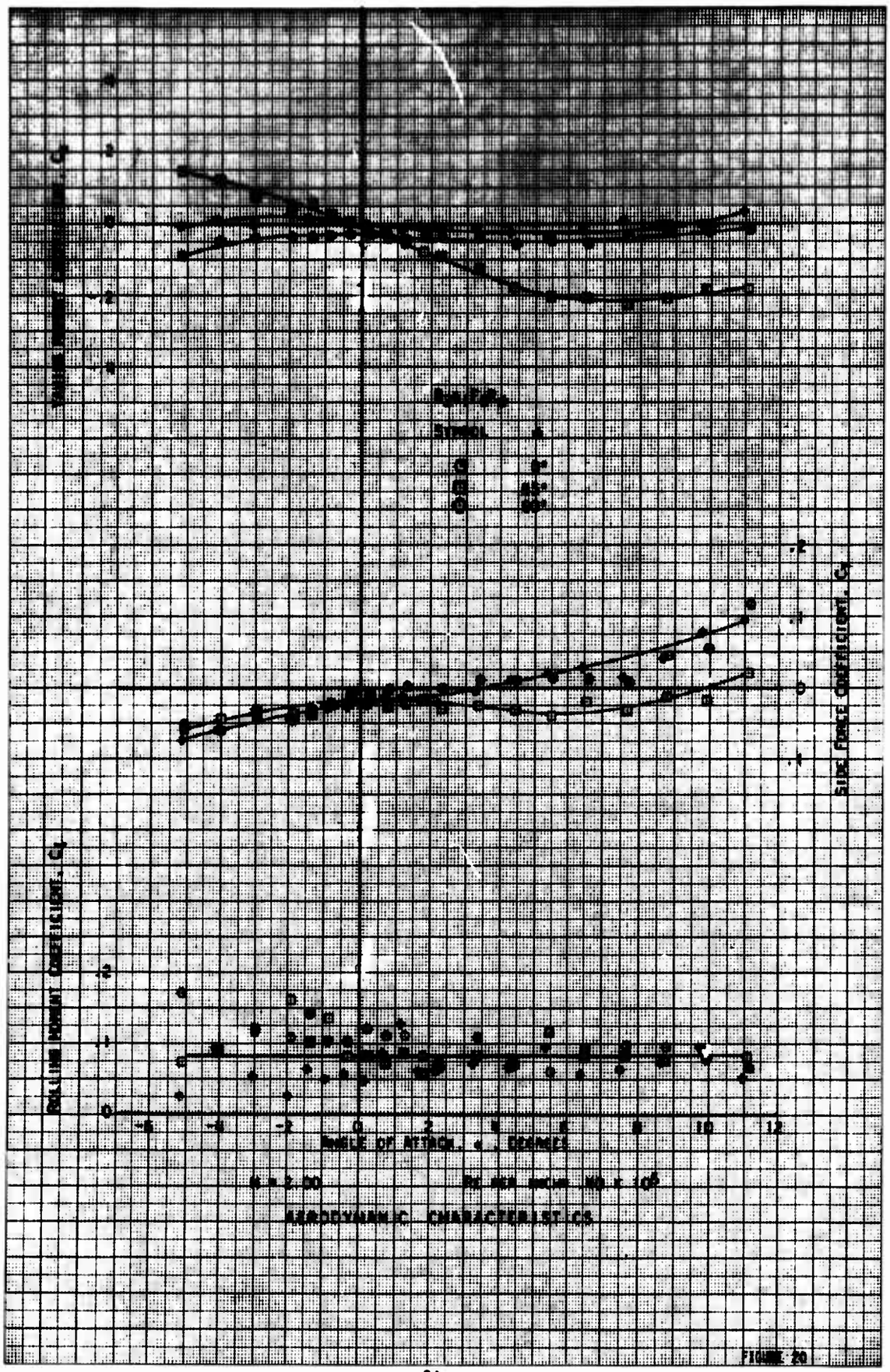
ROLLING MOMENT COEFFICIENT, C_l
SIDE FORCE COEFFICIENT, C_Y
ANGLE OF ATTACK, α, DEGREES
M = 2.30
AERODYNAMIC CHARACTERISTICS

FIGURE 20

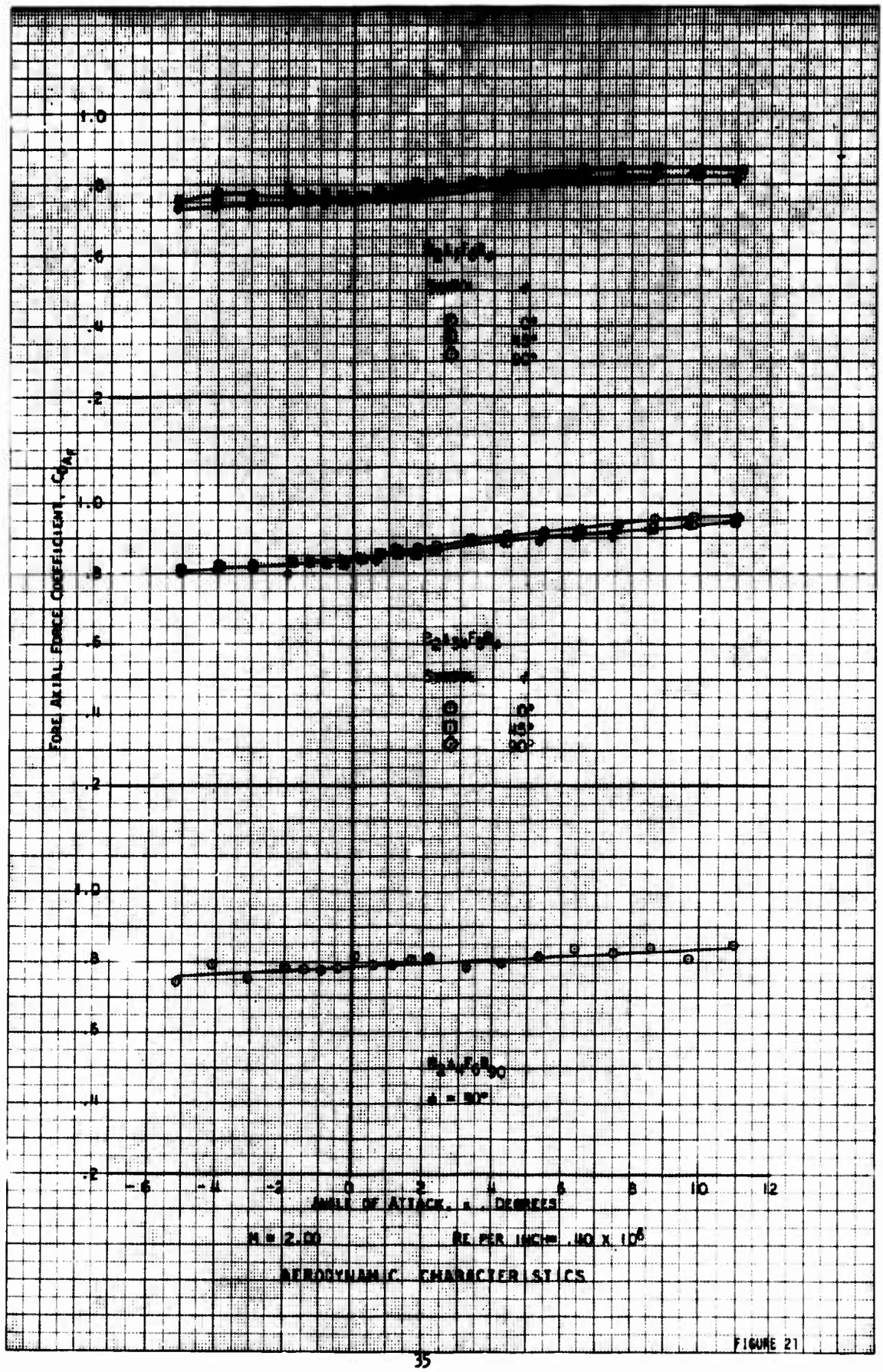
FORE AXIAL FORCE COEFFICIENT, C_{A_F}
1.0
.9
.8
.7
.6
.5
.4
.3
.2
.1
0
.1
.2
1.0
.9
.8
.7
.6
.5
.4
.3
.2
-6
-4
-2
0
2
4
6
8
10
12
ANGLE OF ATTACK, α, DEGREES
M = 2.00
RE PER INCH = .140 X 10^6
AERODYNAMIC CHARACTERISTICS

FIGURE 21

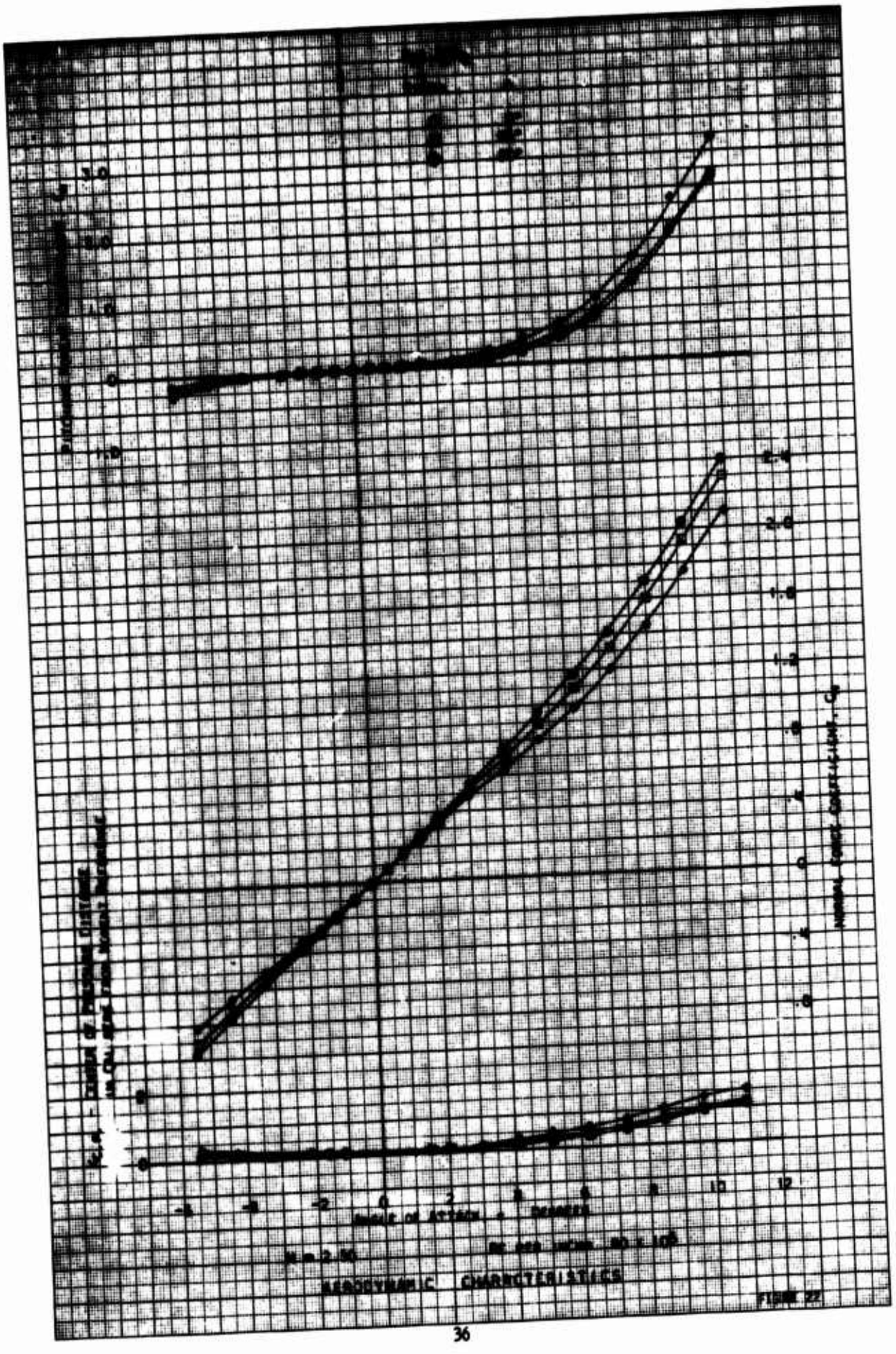
AERODYNAMIC CHARACTERISTICS

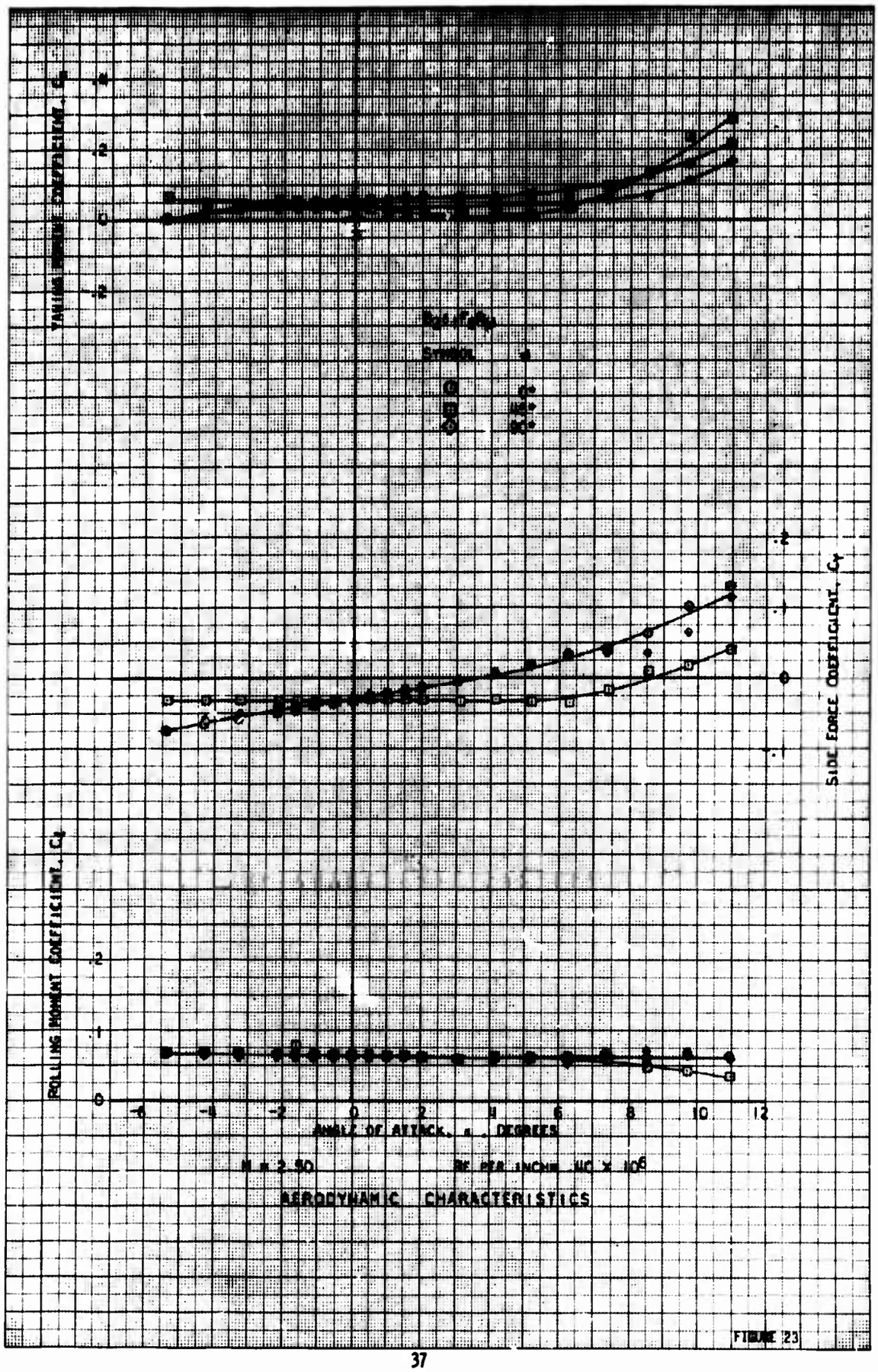
YAWING MOMENT COEFFICIENT, C_n
Body Axis Symbols
SIDE FORCE COEFFICIENT, C_Y
ROLLING MOMENT COEFFICIENT, C_l
ANGLE OF ATTACK, α, DEGREES
M = 2.90
RE PER INCH .MC x 10^6
AERODYNAMIC CHARACTERISTICS

FIGURE 23

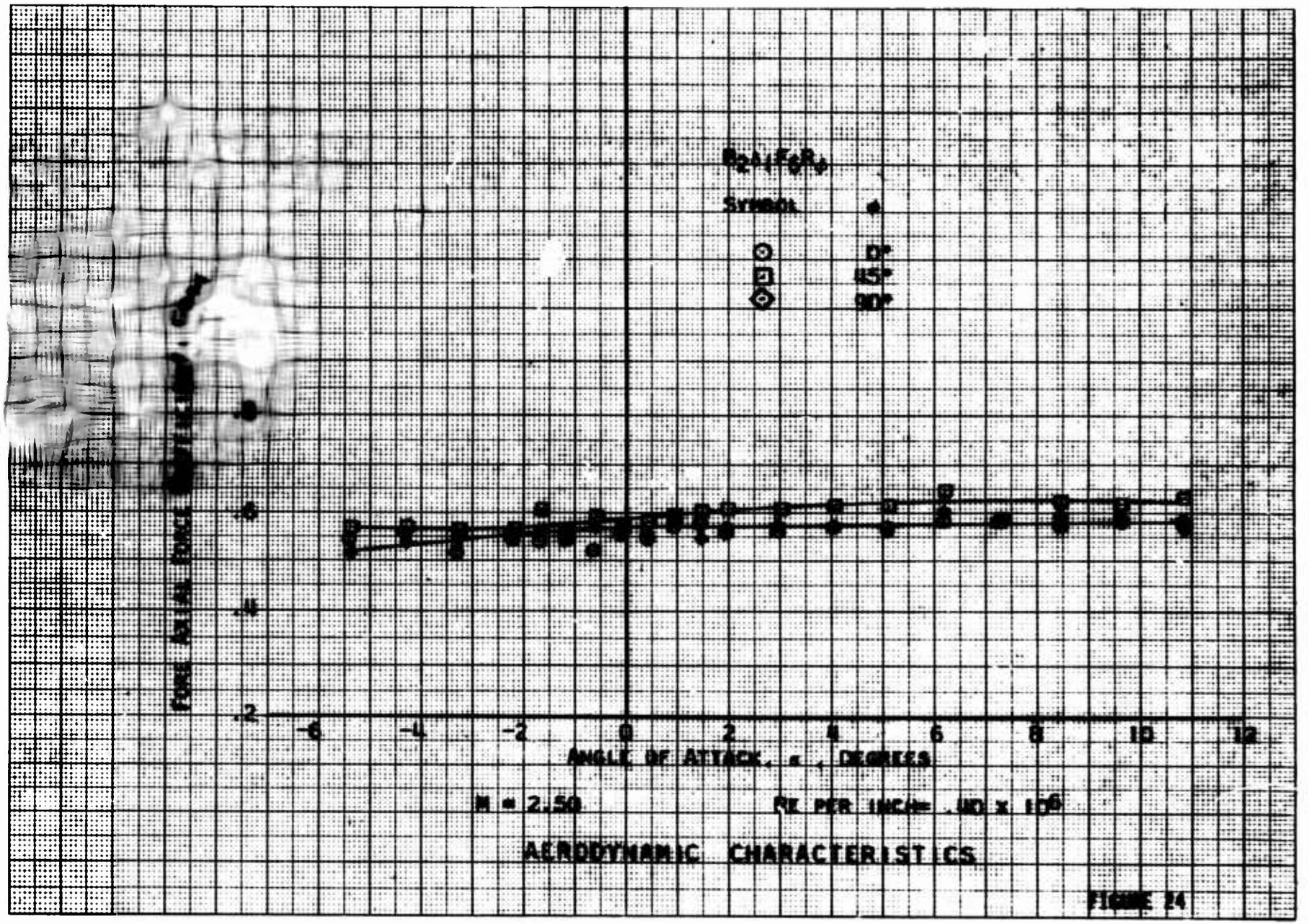

AERODYNAMIC CHARACTERISTICS

FIGURE 24

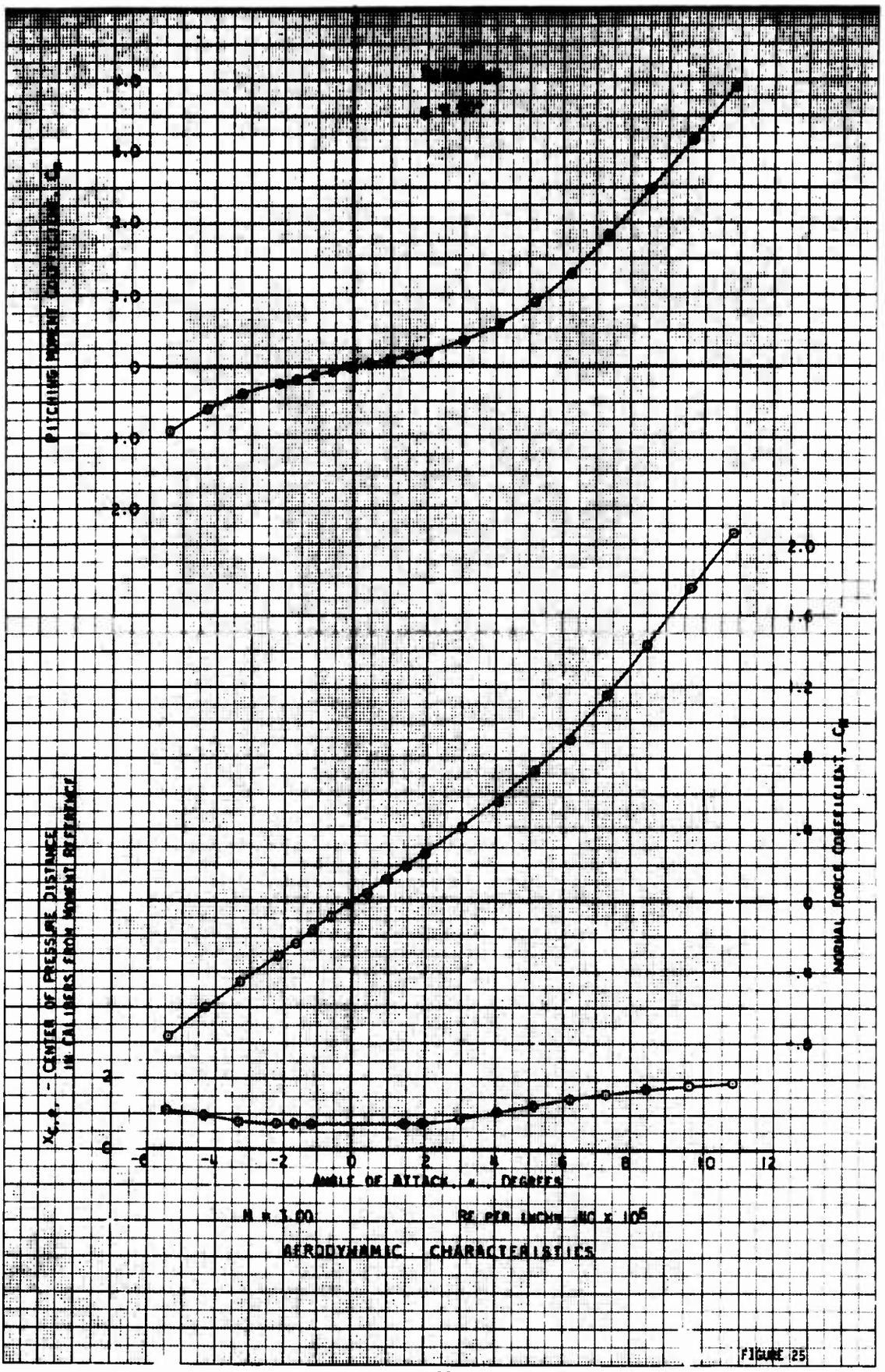
PITCHING MOMENT COEFFICIENT, C_m
$X_{c.p.}$ - CENTER OF PRESSURE DISTANCE IN CALIBERS FROM MOMENT REFERENCE
NORMAL FORCE COEFFICIENT, C_N
2.0
1.0
0
-1.0
-2.0
.2
0
-.2
-.4
-.6
-.8
-6
-4
-2
0
2
4
6
8
10
12
ANGLE OF ATTACK, α, DEGREES
M = 3.00
RE PER INCH, 80 x 10^6
AERODYNAMIC CHARACTERISTICS

FIGURE 25

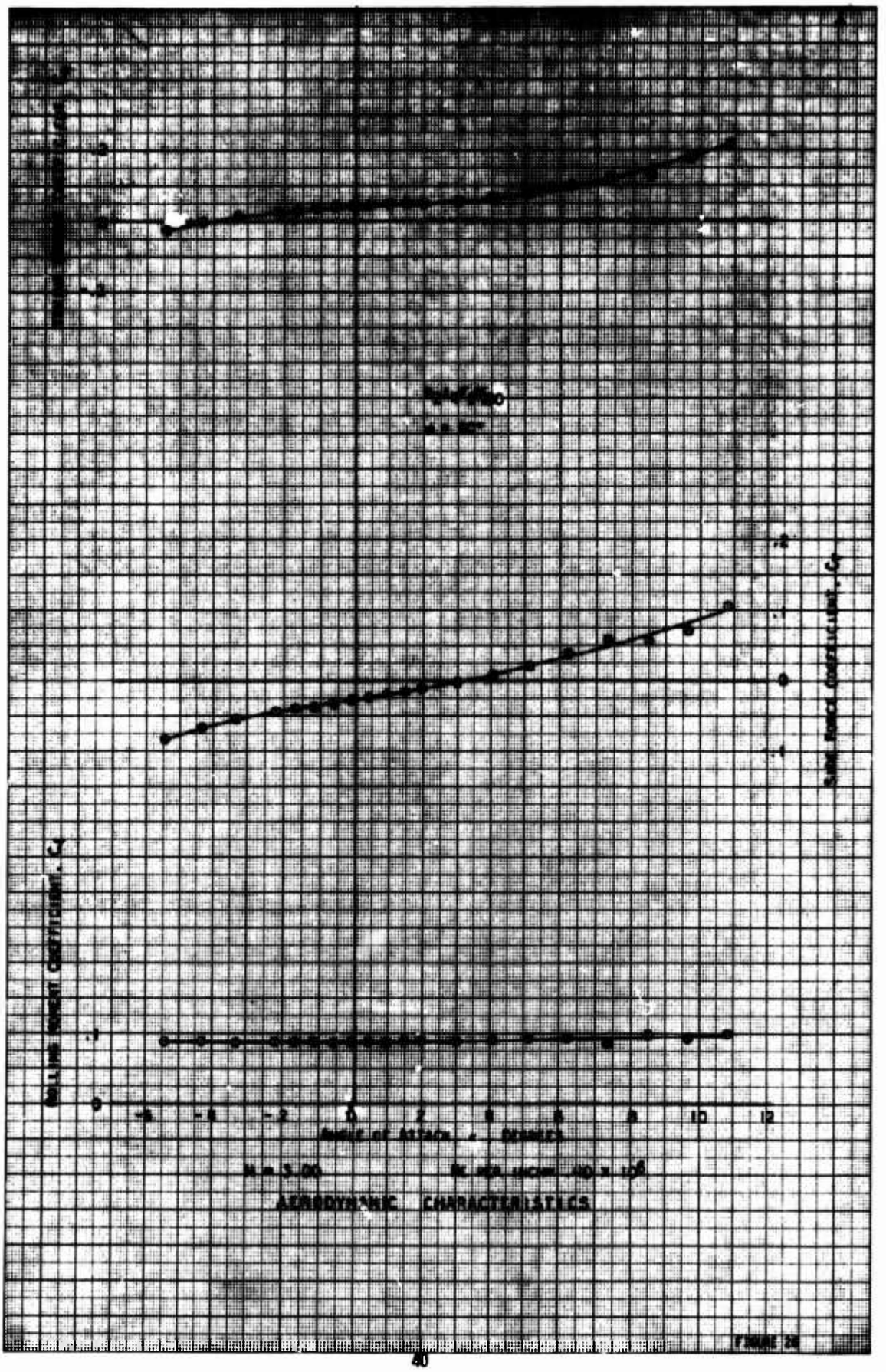
Axial-force coefficient, C_A
Normal-force coefficient, C_N
Pitching-moment coefficient, C_m
Angle of attack, α, degrees
$M_\infty = 3.00$
R_{∞} per inch $= 10 \times 10^6$
AERODYNAMIC CHARACTERISTICS

FIGURE 28

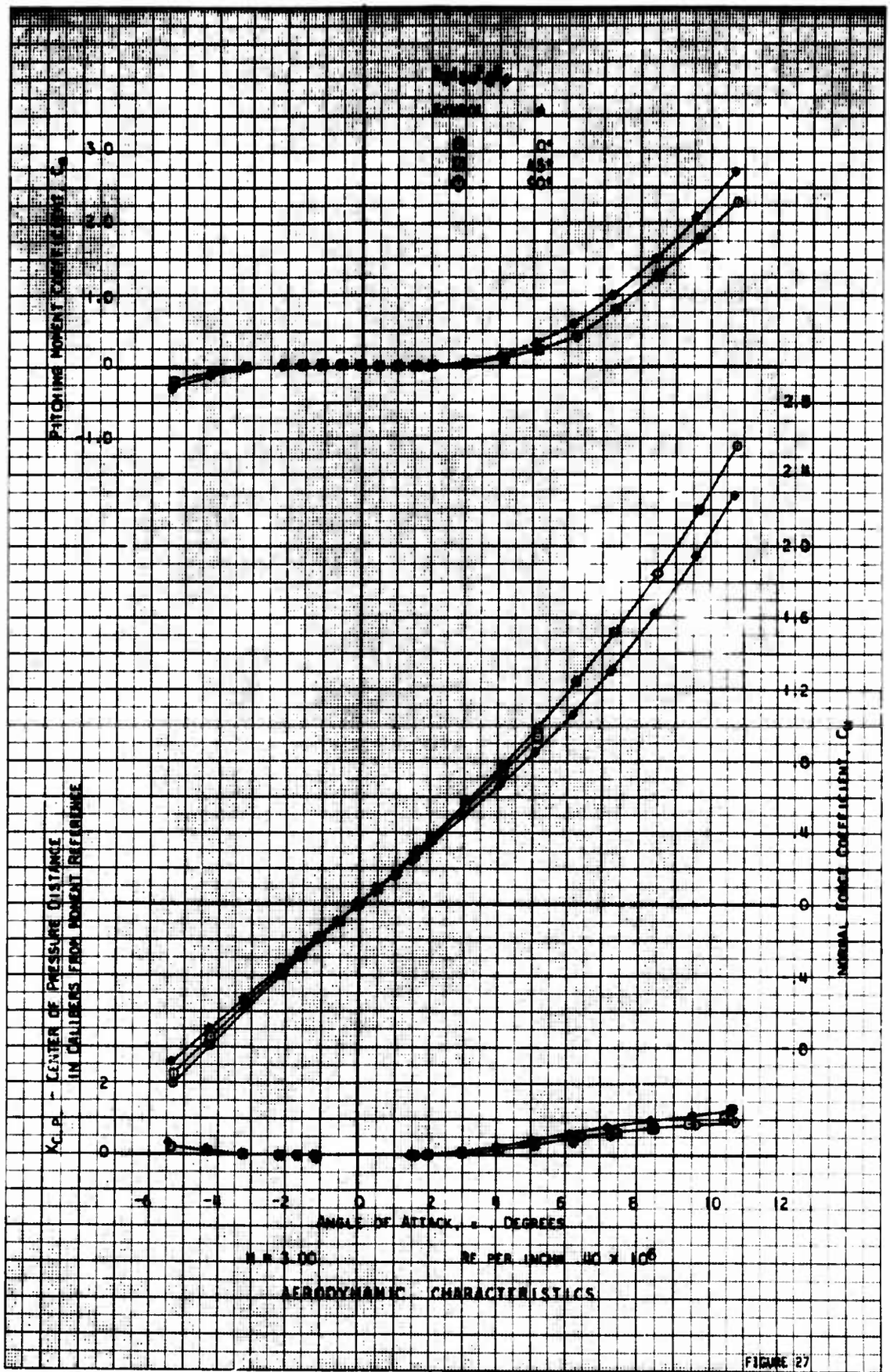
PITCHING MOMENT COEFFICIENT C_m
$X_{C.P.}$ - CENTER OF PRESSURE DISTANCE IN CALIBERS FROM MOMENT REFERENCE
NORMAL FORCE COEFFICIENT C_N
ANGLE OF ATTACK, α, DEGREES
M = 3.00
RE PER INCH 10 x 10^6
AERODYNAMIC CHARACTERISTICS

FIGURE 27

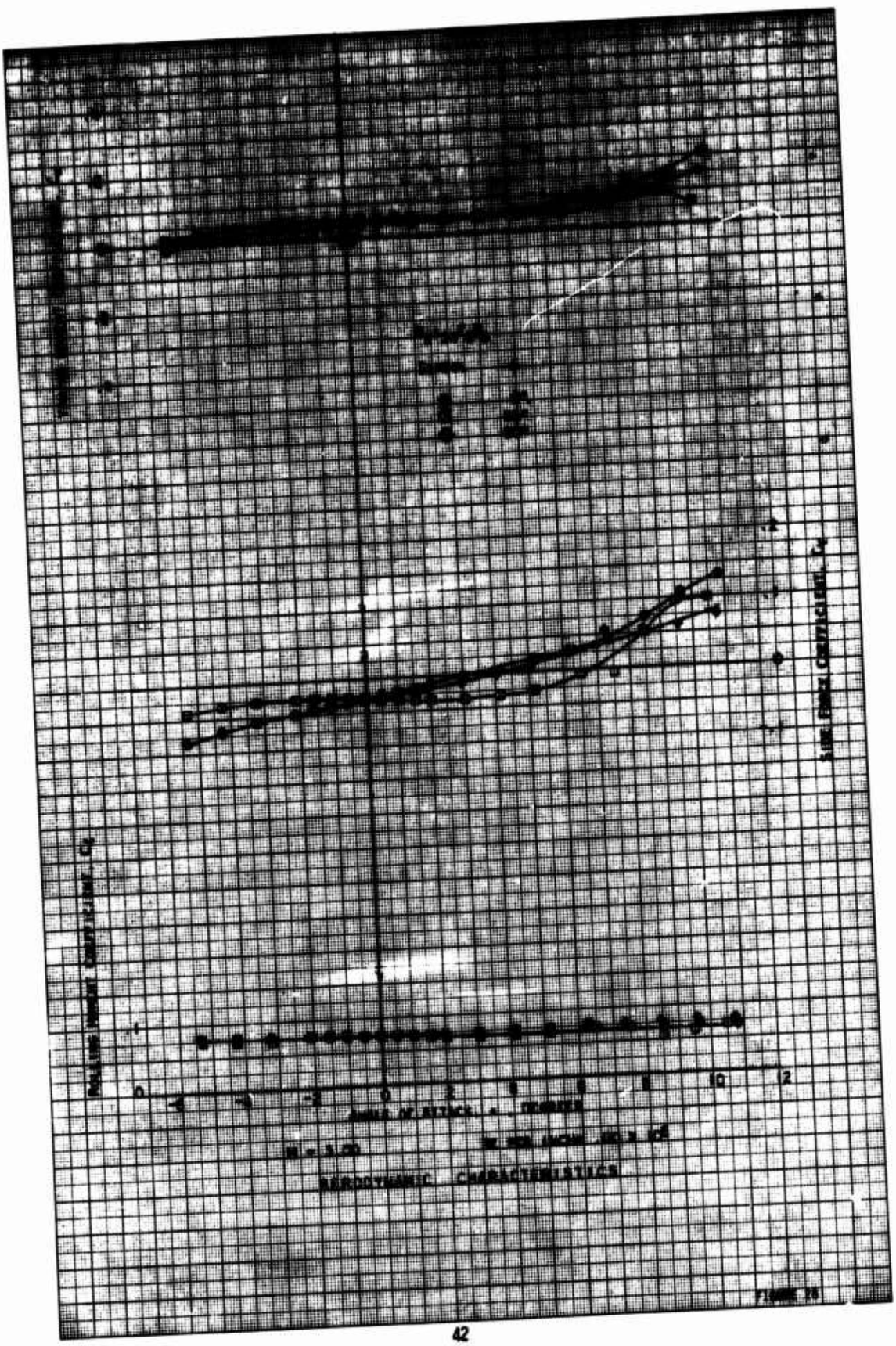
AERODYNAMIC CHARACTERISTICS

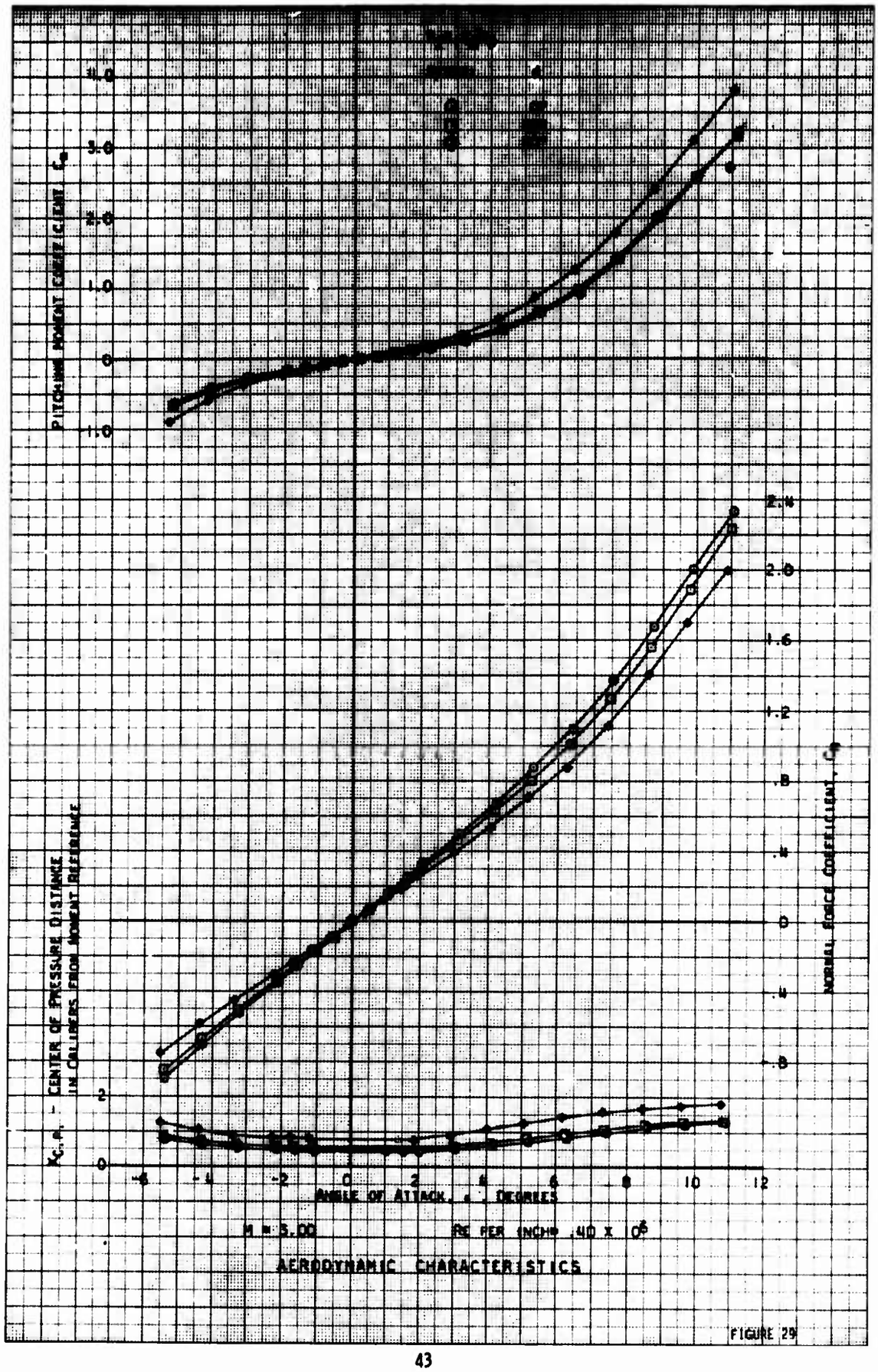
PITCHING MOMENT COEFFICIENT C_m
$X_{C.P.}$ - CENTER OF PRESSURE DISTANCE IN CALIBERS FROM MOMENT REFERENCE
NORMAL FORCE COEFFICIENT C_N
ANGLE OF ATTACK, α, DEGREES
M = 5.00
Re PER INCH = .40 X 10^6
AERODYNAMIC CHARACTERISTICS

FIGURE 29

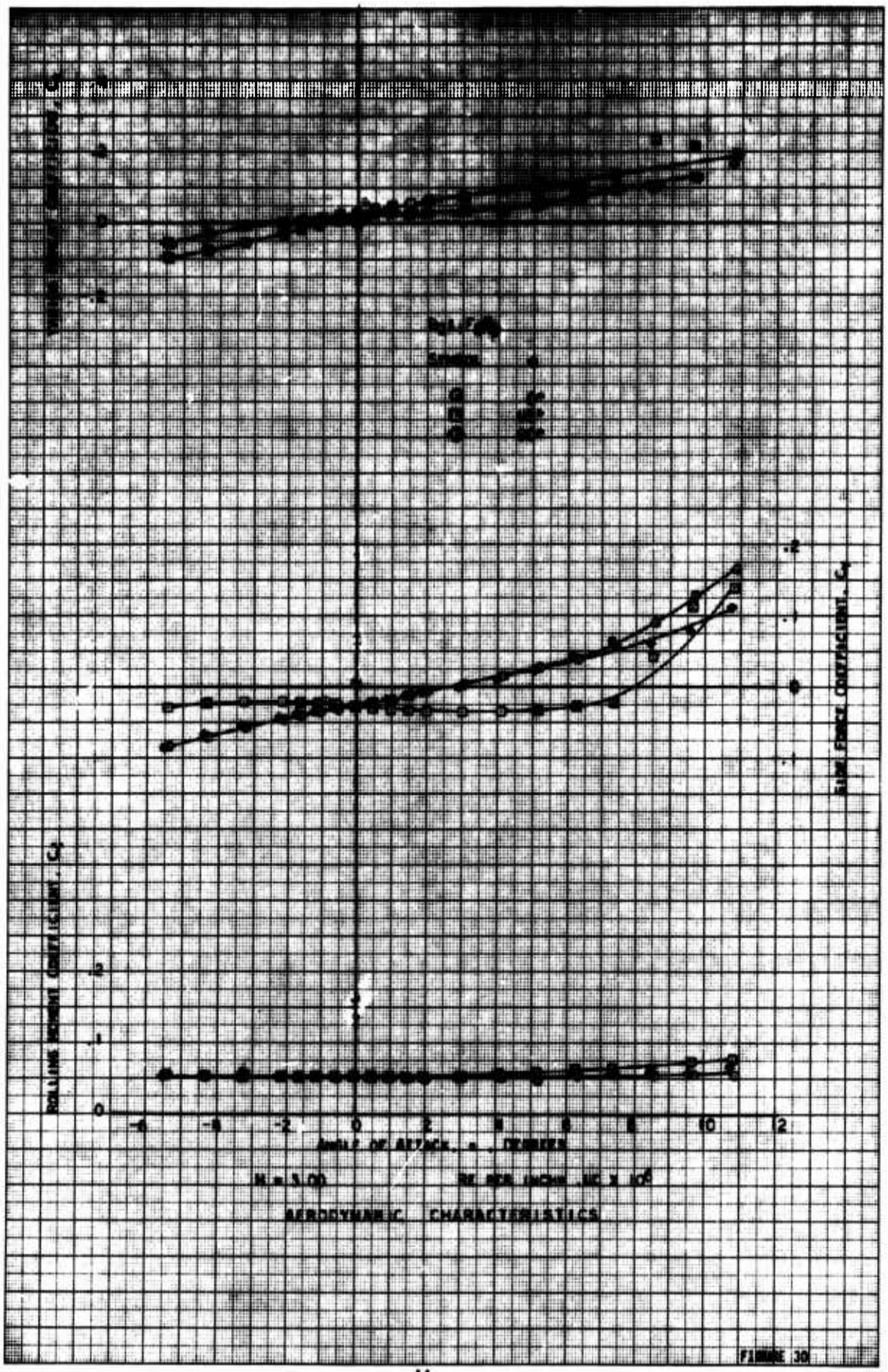
ROLLING MOMENT COEFFICIENT, C_l
SIDE FORCE COEFFICIENT, C_y
0
-4
-8
-2
0
2
4
6
8
10
12
M = 3.00
AERODYNAMIC CHARACTERISTICS

FIGURE 30

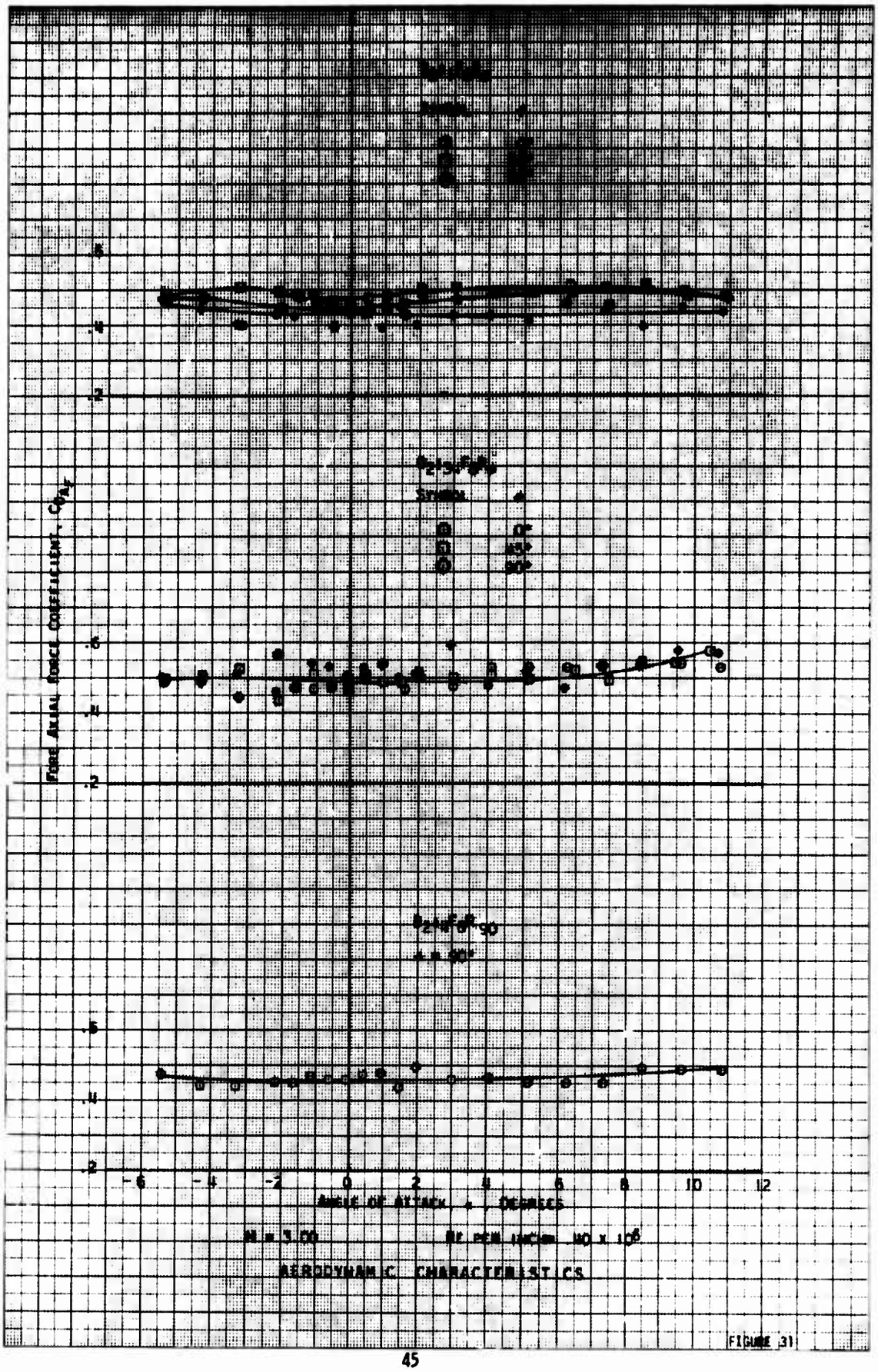
FORE AXIAL FORCE COEFFICIENT, C_{A_F}
.8
.6
.4
.2
-.2
-.4
-.6
-.8
-6
-4
-2
0
2
4
6
8
10
12
ANGLE OF ATTACK, α, DEGREES
M = 3.00
RE PER INCH, 40 x 10^6
AERODYNAMIC CHARACTERISTICS

FIGURE 31

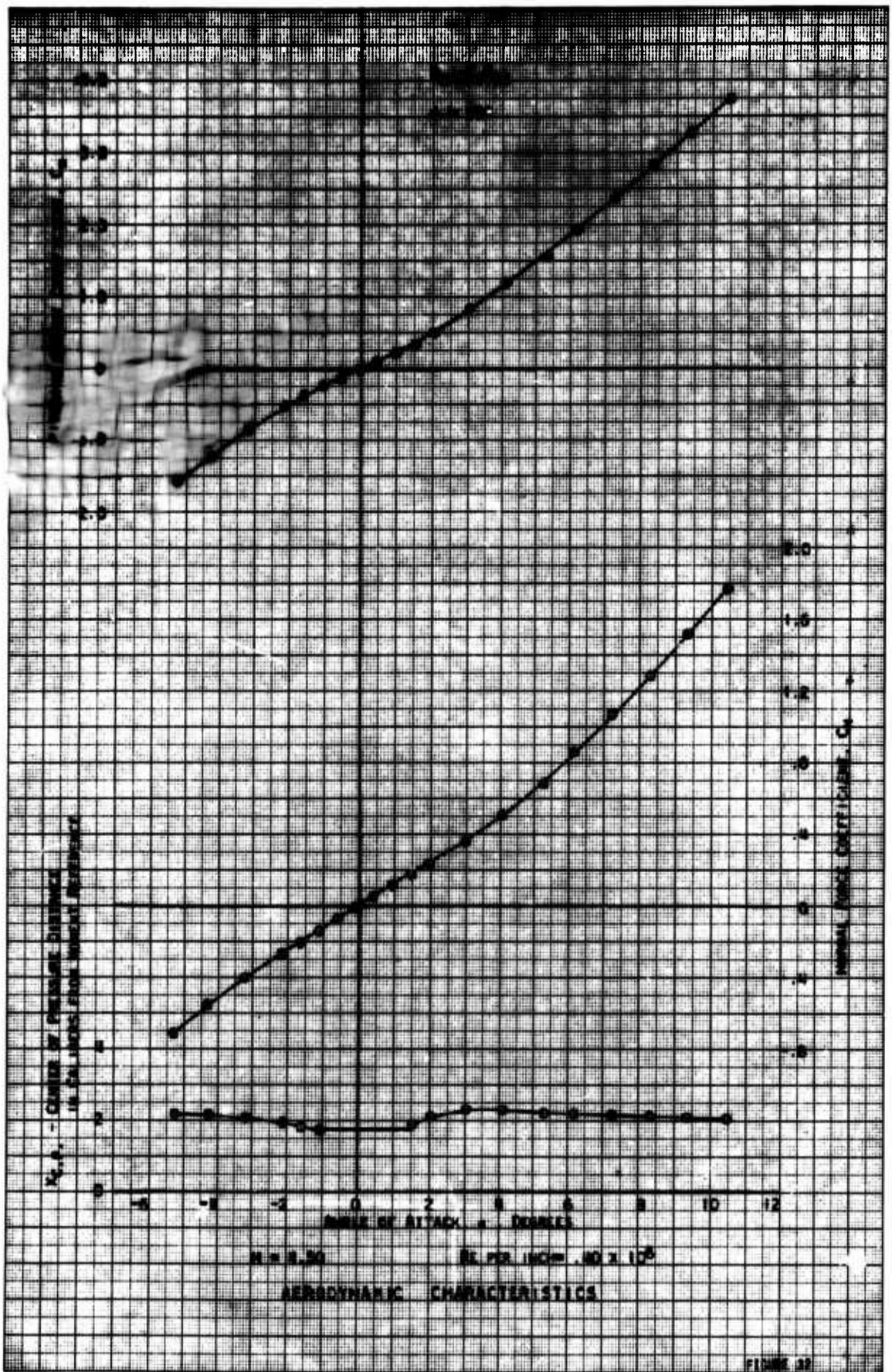
ANGLE OF ATTACK, α, DEGREES
M = 0.30
RE. PER INCH = .40 X 10⁶
AERODYNAMIC CHARACTERISTICS

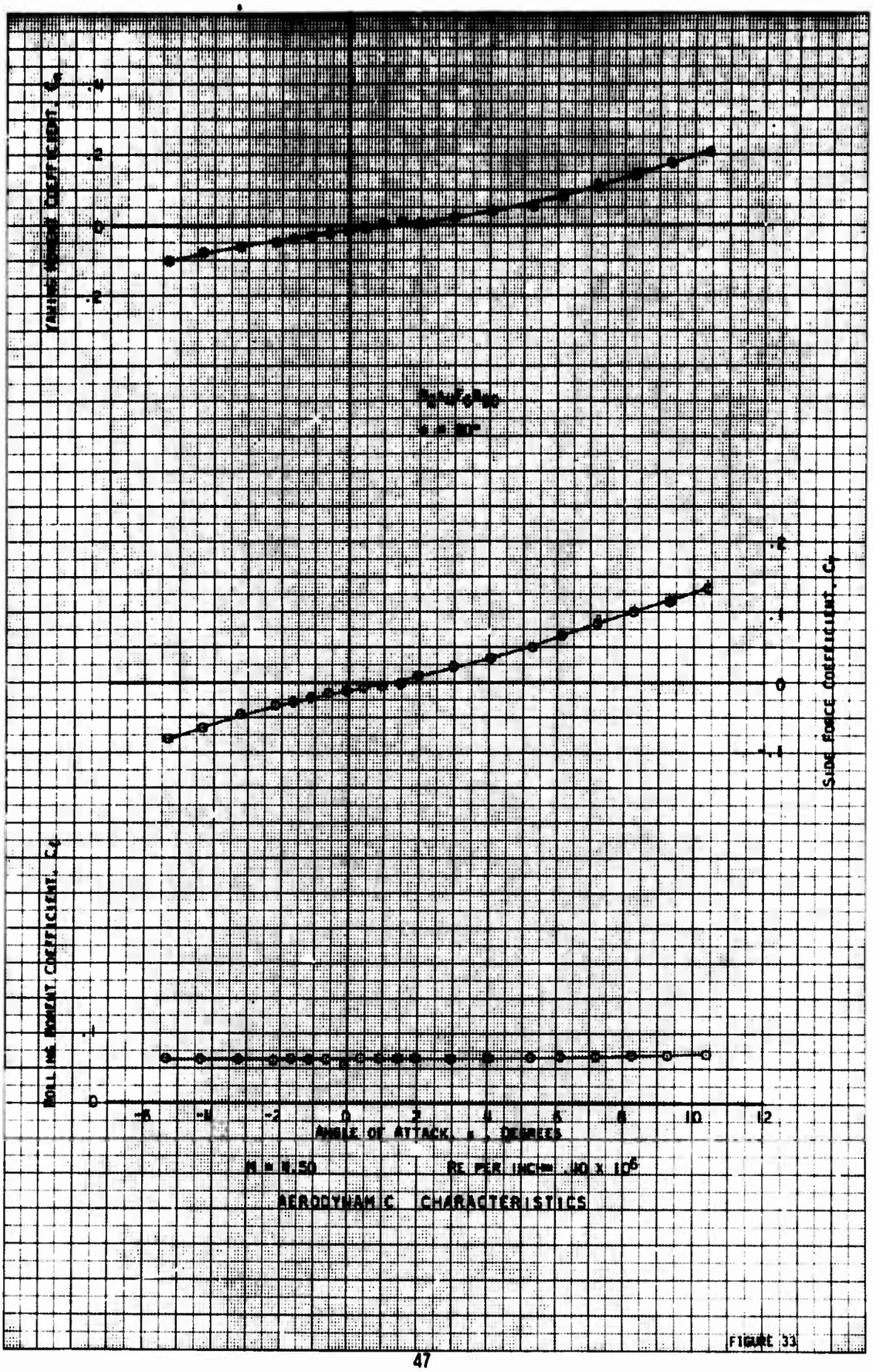
ROLLING MOMENT COEFFICIENT, C_l
YAWING MOMENT COEFFICIENT, C_n
SIDE FORCE COEFFICIENT, C_y
ANGLE OF ATTACK, α, DEGREES
M = 8.50
RE PER INCH = 10 X 10^6
AERODYNAMIC CHARACTERISTICS

FIGURE 33

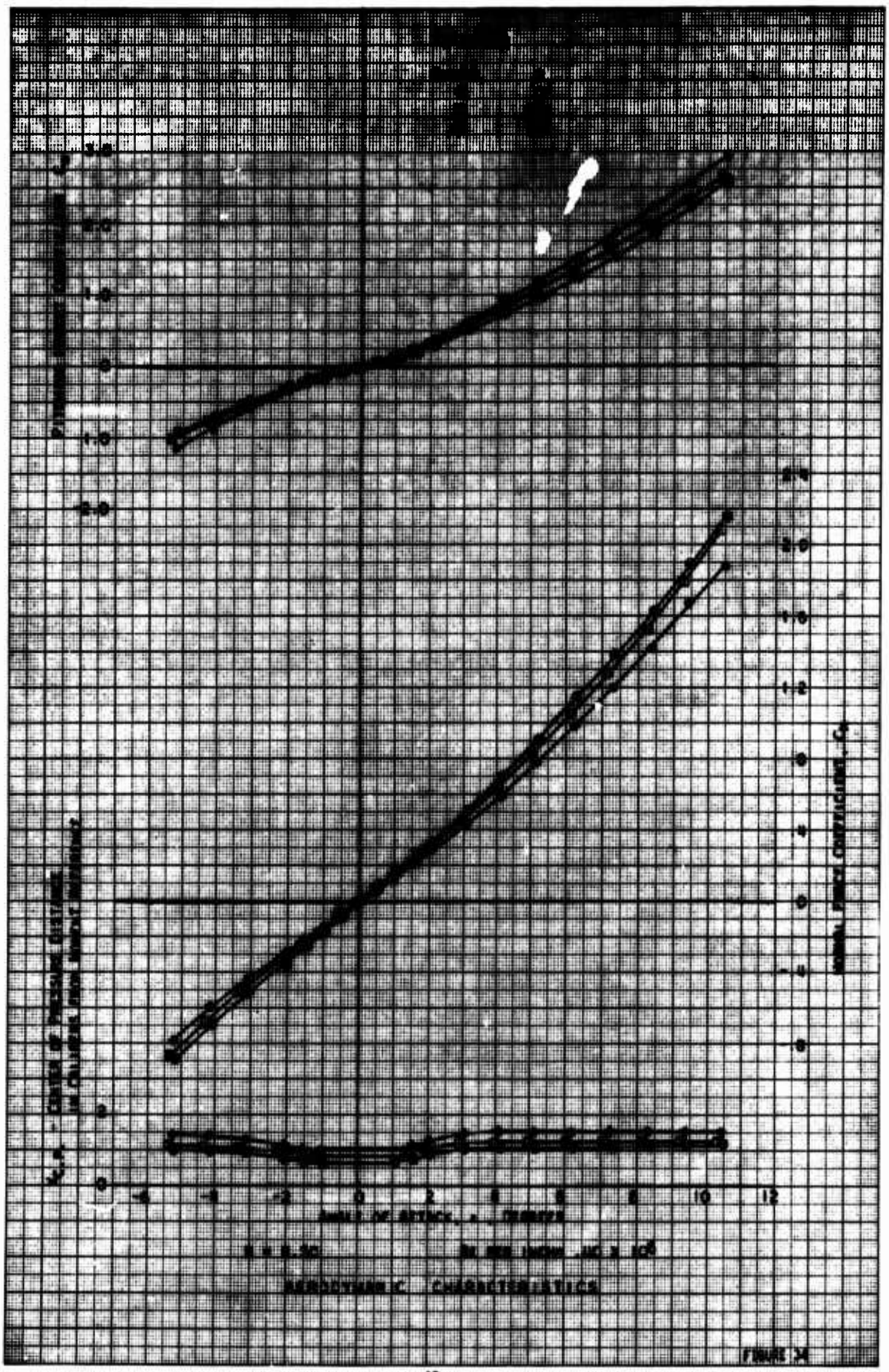

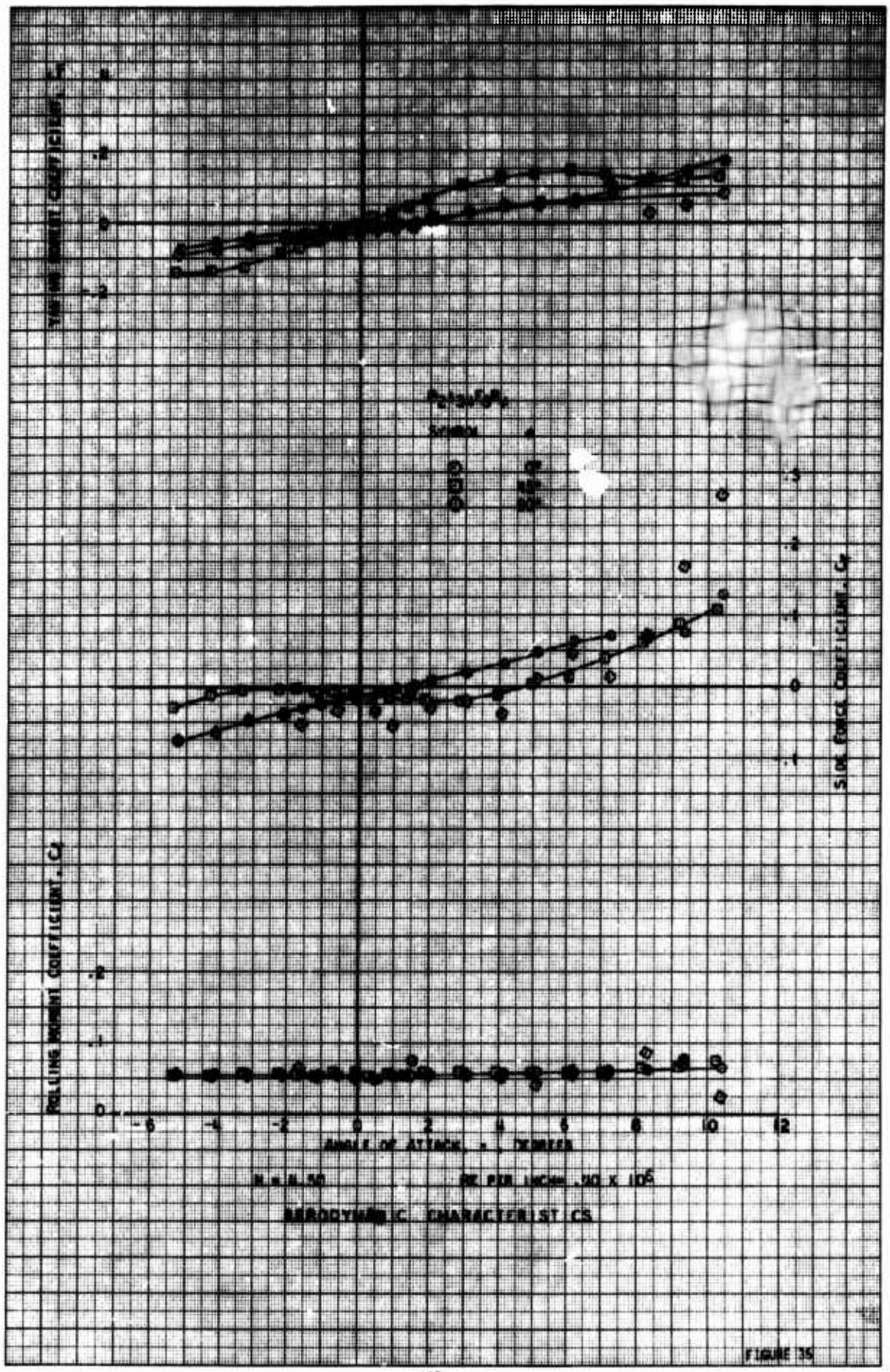
ROLLING MOMENT COEFFICIENT, C_l
SIDE FORCE COEFFICIENT, C_Y
ANGLE OF ATTACK, α, DEGREES
M = 0.50
RE PER INCH, .90 X 10^6
AERODYNAMIC CHARACTERISTICS

FIGURE 35

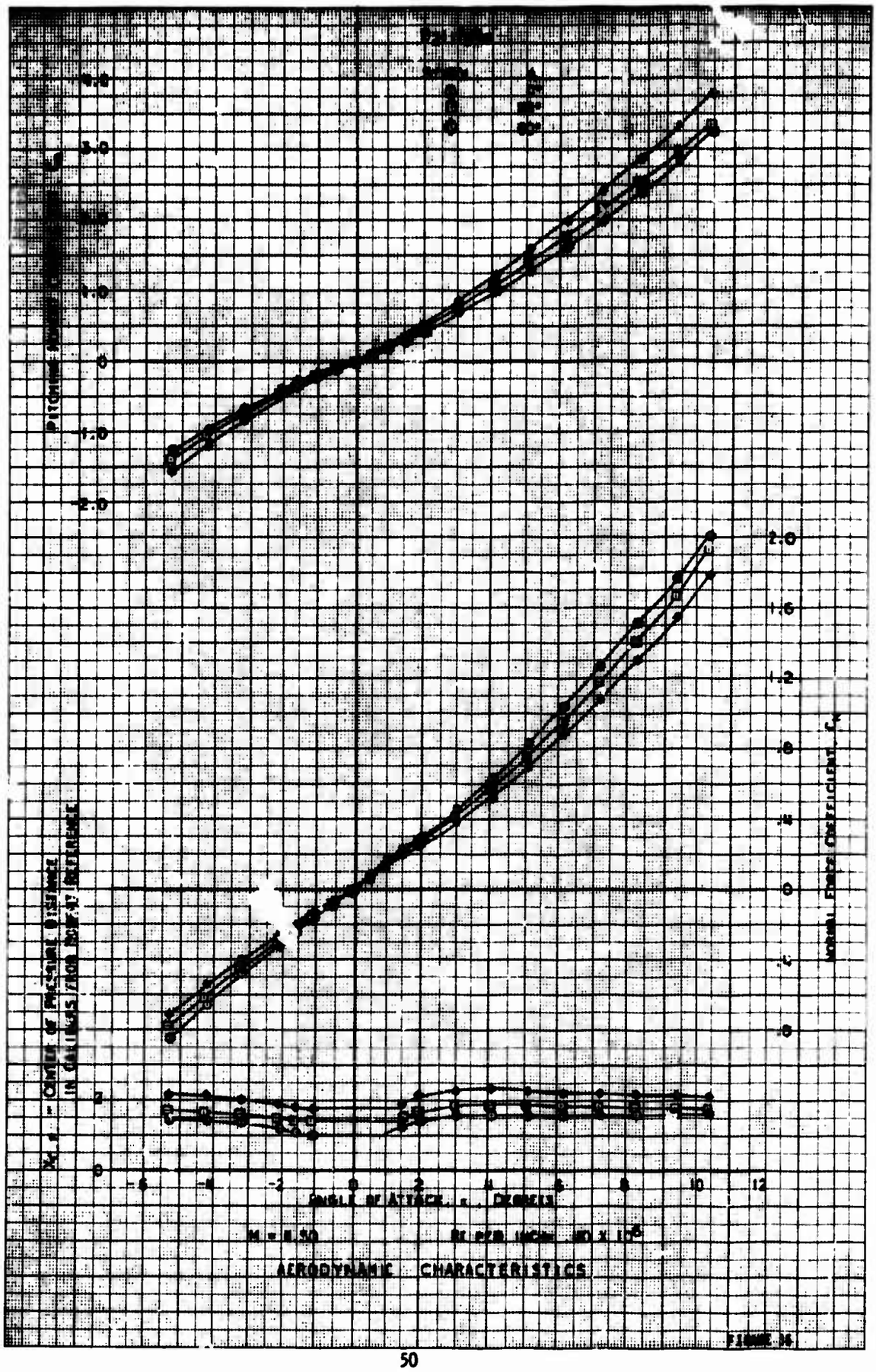
AERODYNAMIC CHARACTERISTICS

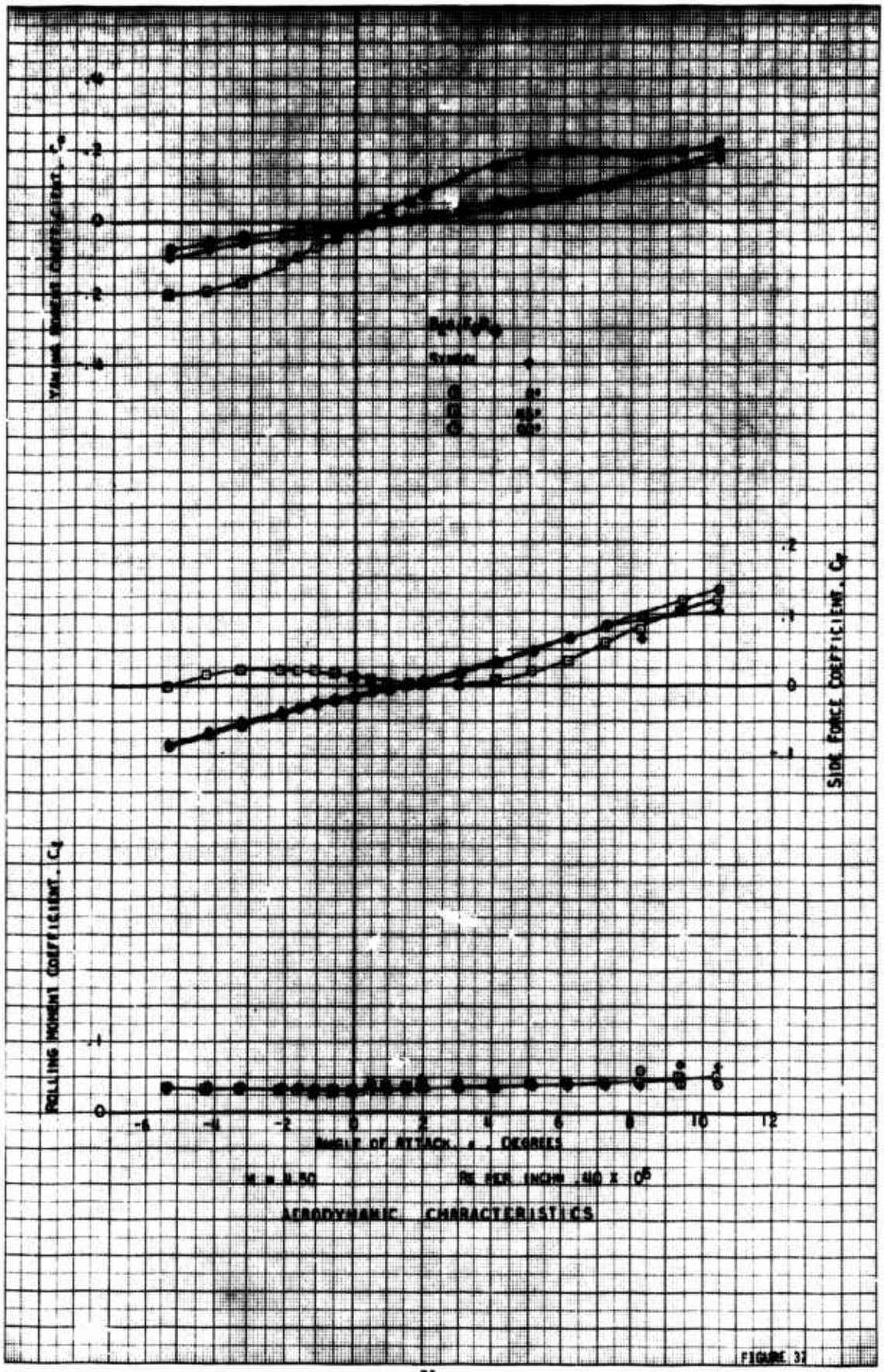
YAWING MOMENT COEFFICIENT, C_n
SIDE FORCE COEFFICIENT, C_y
ROLLING MOMENT COEFFICIENT, C_l
ANGLE OF ATTACK, α, DEGREES
M = 0.50
RE PER INCH .40 X 10^6
AERODYNAMIC CHARACTERISTICS

FIGURE 31

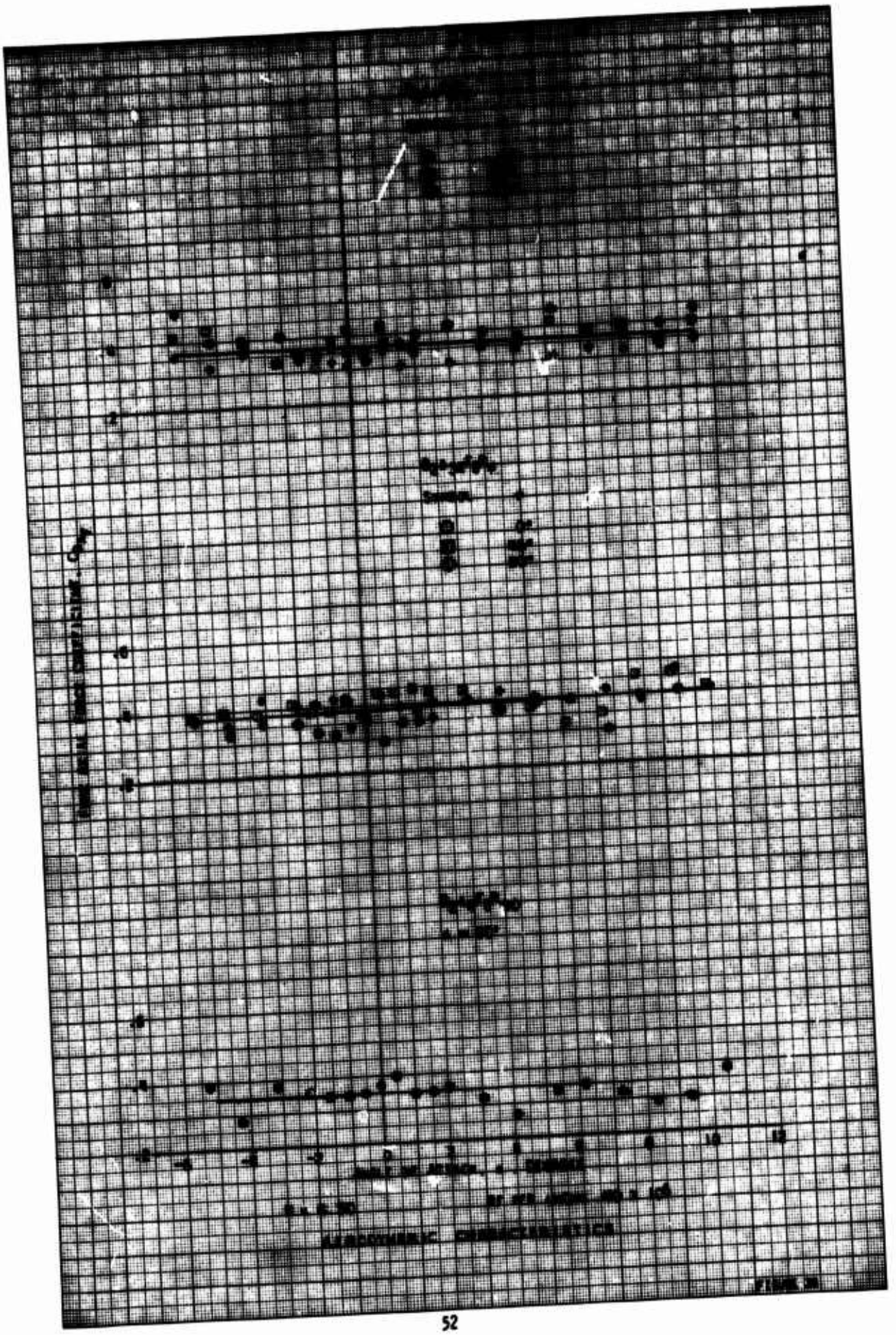

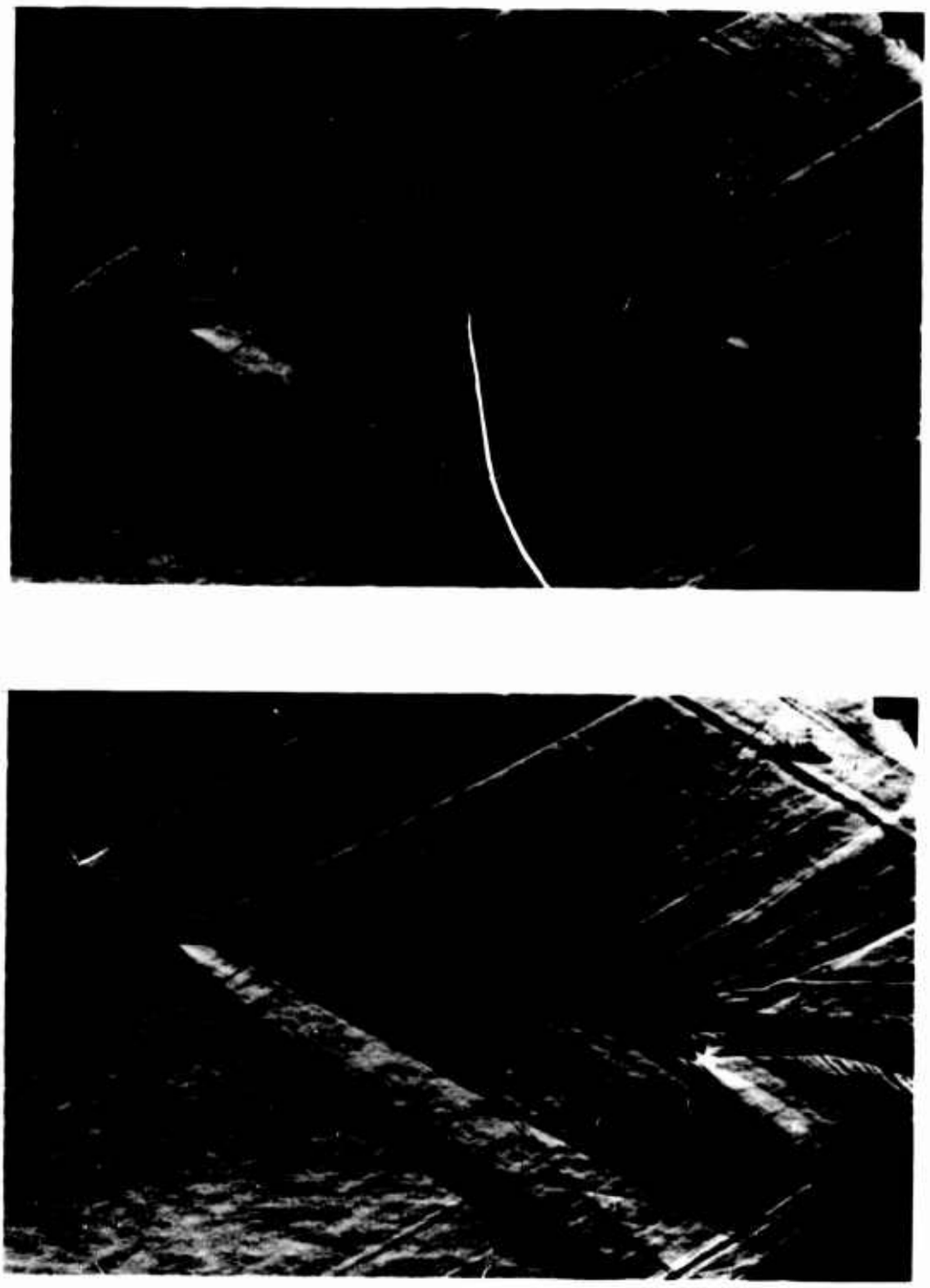

Figure No. 39 - Small fin configuration at $\phi = 90^{\circ}$ and $\alpha = 0^{\circ}$ and 6°.
Flow conditions; M = 2.0 and $Re/\ell = 0.40 \times 10^{6}$.

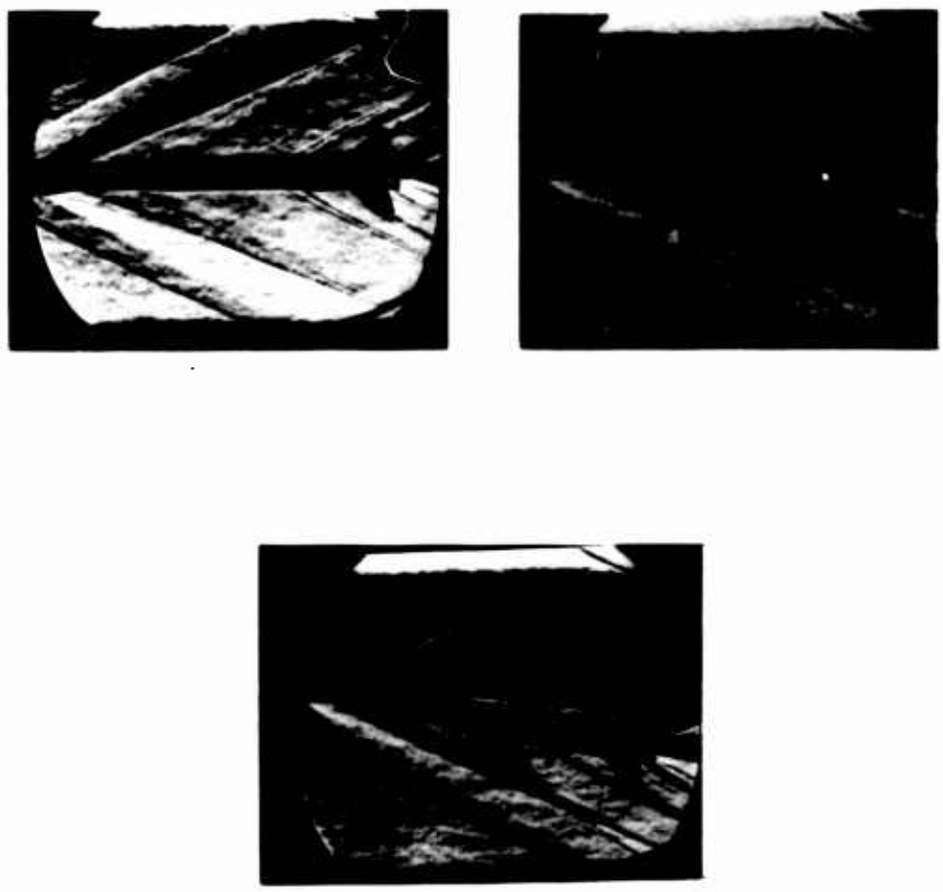

Figure No. 40 - Small fin configurations at $\phi = 45^{\circ}$ and $\alpha = 0^{\circ}$, 6° and 10°. Flow conditions; M = 2.50 and $Re/\ell = 0.40 \times 10^{6}$.

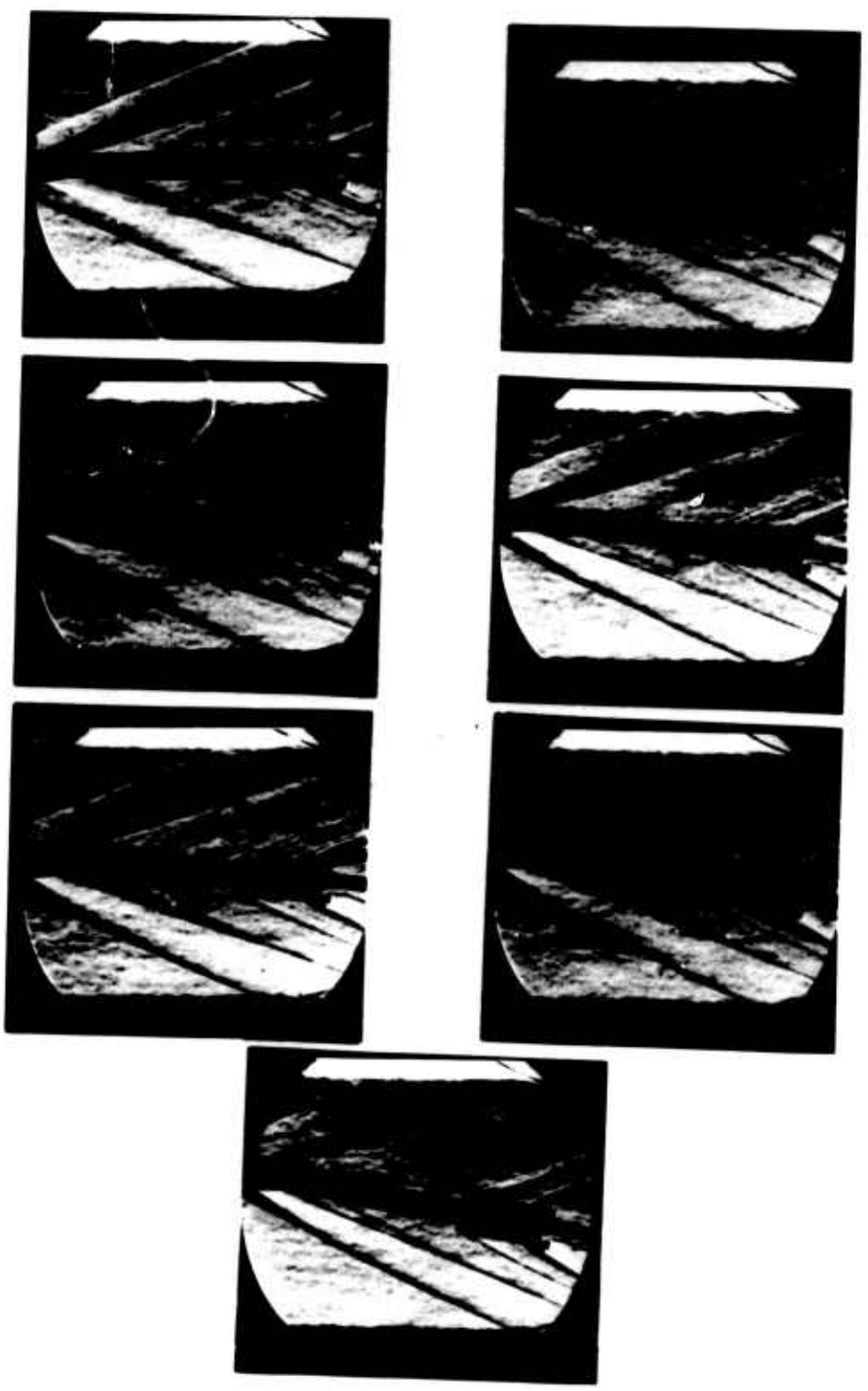

Figure No. 41 - Small fin configuration at $\phi = 90^{\circ}$ and $\alpha = 0, 2, 3, 4, 5, 6$ and 8°. Flow conditions: $M = 3.0$ and $Re/\ell = 0.4 \times 10^{6}$.

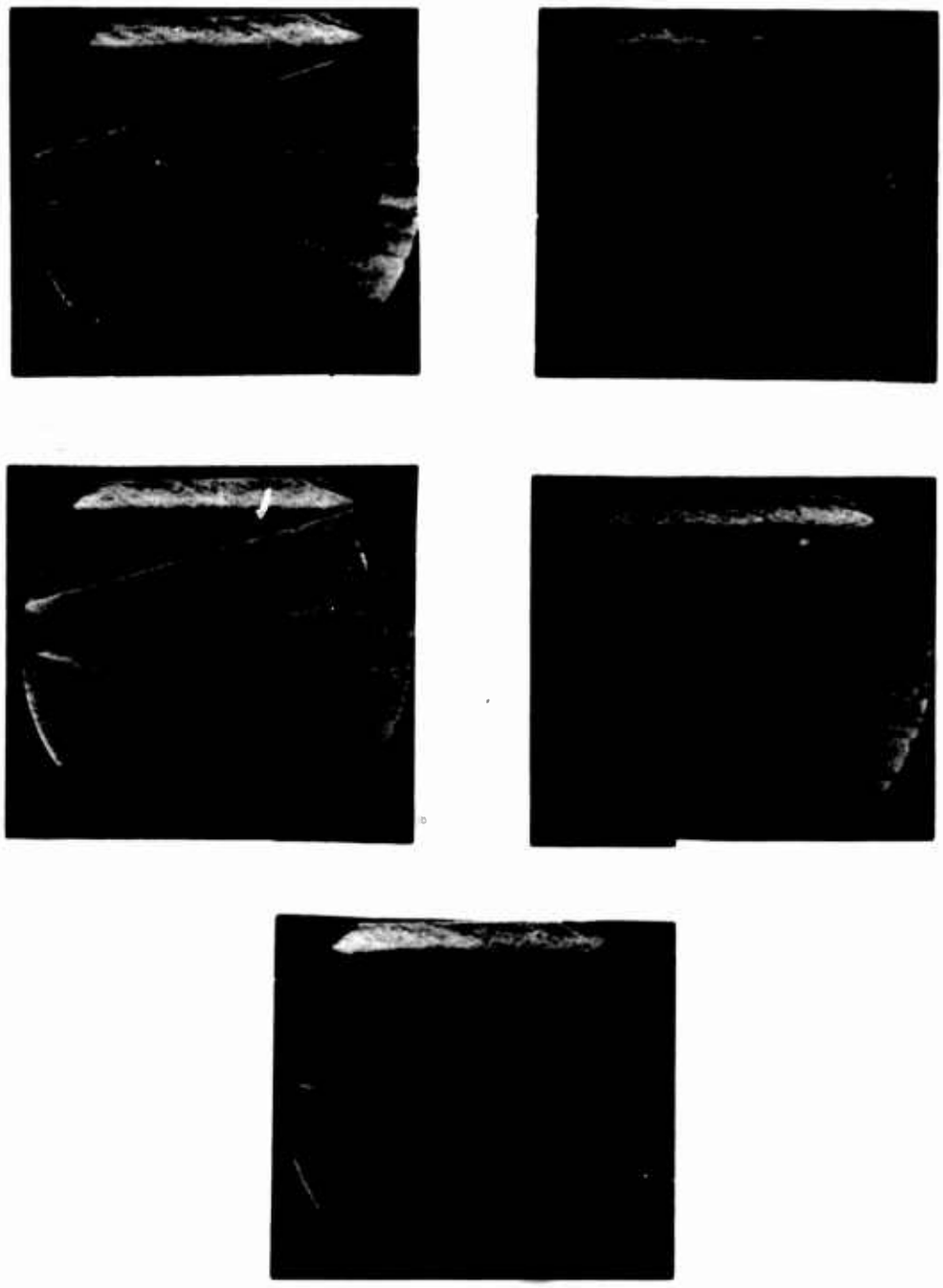

Figure No. 42 - Small fin configuration at $\phi = 90^{\circ}$ and $\alpha = 0, 2, 3, 4$ and 5°. Flow conditions; $M = 4.5$ and $Re/\ell = 0.4 \times 10^{6}$.

Unclassified
Security Classification

DOCUMENT CONTROL DATA - R & D

(Security classification of title, body of abstract and indexing annotation must be entered when the overall report is classified)

1. ORIGINATING ACTIVITY (Corporate author) U.S. Army Ballistic Research Laboratories Aberdeen Proving Ground, Maryland	2a. REPORT SECURITY CLASSIFICATION Unclassified 2b. GROUP

3. REPORT TITLE

SUPERSONIC WIND TUNNEL TESTS OF THE THREE-STAGE TARGET MISSILE ARPAT

4. DESCRIPTIVE NOTES (Type of report and inclusive dates)

5. AUTHOR(S) (First name, middle initial, last name)

Joseph M. Hughes

6. REPORT DATE	7a. TOTAL NO. OF PAGES	7b. NO. OF REFS
March 1968	58	

8a. CONTRACT OR GRANT NO.	9a. ORIGINATOR'S REPORT NUMBER(S)
b. PROJECT NO. 1T222901A201	Memorandum Report No. 1915
c.	9b. OTHER REPORT NO(S) (Any other numbers that may be assigned this report)
d.	

10. DISTRIBUTION STATEMENT

This document has been approved for public release and sale; its distribution is unlimited.

11. SUPPLEMENTARY NOTES	12. SPONSORING MILITARY ACTIVITY
	U.S. Army Materiel Command Washington, D.C.

13. ABSTRACT

Wind tunnel tests were performed on a four-percent scale model of the ARPAT Target Vehicle in the Ballistic Research Laboratories' Supersonic Wind Tunnels at Aberdeen Proving Ground, Maryland. Fins of varying area and deflection were tested at Mach numbers of 2.00, 2.50, 3.00 and 4.50. The dynamic roll rate, the pitching moment coefficient, the normal and drag force coefficients, and the center of pressure positions were determined through an angle of attack range. The results are presented and summarized in this report.

DD FORM 1 NOV 68 1473 REPLACES DD FORM 1473, 1 JAN 64, WHICH IS OBSOLETE FOR ARMY USE.

Unclassified
Security Classification

14. KEY WORDS	LINK A		LINK B		LINK C	
	ROLE	WT	ROLE	WT	ROLE	WT
ARPAT						
Wind Tunnel Test						
Missile						
Supersonic Aerodynamics						
Experimental Aerodynamics						